SCIENTIFIC REPORTS
nature research

OPEN

Phenylethylamides derived from bacterial secondary metabolites specifically inhibit an insect serotonin receptor

Ariful Hasan[1], Hyun-Suk Yeom[2], Jaewook Ryu[2], Helge B. Bode[3] & Yonggyun Kim[1*]

Serotonin (5-hydroxytryptamine: 5-HT) is a biogenic monoamine that mediates immune responses and modulates nerve signal in insects. *Se-5HTR*, a specific receptor of serotonin, has been identified in the beet armyworm, *Spodoptera exigua*. It is classified into subtype 7 among known 5HTRs. *Se-5HTR* was expressed in all developmental stages of *S. exigua*. It was expressed in all tested tissues of larval stage. Its expression was up-regulated in hemocytes and fat body in response to immune challenge. RNA interference (RNAi) of *Se-5HTR* exhibited significant immunosuppression by preventing cellular immune responses such as phagocytosis and nodulation. Treatment with an inhibitor (SB-269970) specific to 5HTR subtype 7 resulted in significant immunosuppression. Furthermore, knockout mutant of *Se-5HTR* by CRISPR-Cas9 led to significant reduction of phagocytotic activity of *S. exigua* hemocytes. Such immunosuppression was also induced by bacterial secondary metabolites derived from *Xenorhabdus* and *Photorhabdus*. To determine specific bacterial metabolites inhibiting Se-5HTR, this study screened 37 bacterial secondary metabolites with respect to cellular immune responses associated with Se-5HTR and selected 10 potent inhibitors. These 10 selected compounds competitively inhibited cellular immune responses against 5-HT and shared phenylethylamide (PEA) chemical skeleton. Subsequently, 46 PEA derivatives were screened and resulting potent chemicals were used to design a compound to be highly inhibitory against Se-5HTR. The designed compound was chemically synthesized. It showed high immunosuppressive activities along with specific and competitive inhibition activity for Se-5HTR. This study reports the first 5HT receptor from *S. exigua* and provides its specific inhibitor designed from bacterial metabolites and their derivatives.

Serotonin or 5-hydroxytryptamine (5-HT) is a biogenic monoamine found across most phyla of life[1]. This indolamine compound is biosynthesized from tryptophan by successive catalytic activities of tryptophan hydroxylase and aromatic-L-amino acid decarboxylase[2–4] primarily in nervous systems[5,6]. In human and other vertebrates, serotonin is a well-known neurotransmitter involved in mood, appetite, sleep, anxiety, cognition, and psychosis[7–9]. Outside the nervous system, serotonin plays important roles as growth factor and regulator of hemostasis and blood clotting[10,11]. In plants, serotonin is basically involved in stress signaling[12]. Serotonin plays crucial role in physiological and behavioral processes in insects and other invertebrates[13,14]. In *Drosophila melanogaster*, there is evidence that serotonin is required for courtship and mating[15], circadian rhythm[16,17], sleep[18], locomotion[13,19], aggression[20], insulin signaling and growth[21], and phagocytosis[22]. Serotonin is also involved in olfactory processing[23], feeding behavior[19], heart rate[24], and responses to light[25] in *D. melanogaster* larvae.

Serotonin modulates physiological processes by binding to specific receptors. Seven main subtypes of serotonin receptors have been classified in vertebrates[26]. Except 5-HT_3 receptor, the other six classes (5-HT_1, 5-HT_2, 5-HT_4, 5-HT_5, 5-HT_6, and 5-HT_7 receptors) belong to G protein-coupled receptor family[27]. Among these receptors, 5-HT_1 and 5-HT_5 receptors can inhibit cAMP synthesis by preferentially coupling to a trimeric G protein $G_{i/o}$[28]. 5-HT_2 receptor uses $G_{q/11}$ to induce breakdown of inositol phosphates, resulting in an increase in cytosolic

[1]Department of Plant Medicals, College of Life Sciences, Andong National University, Andong, 36729, Korea. [2]Center for Eco-Friendly New Materials, Korea Research Institute of Chemicals Technology, Yuseong, Daejeon, 34114, Korea. [3]Department of Biosciences, Molecular Biotechnology, and Buchmann Institute for Molecular Life Sciences (BMLS), Goethe-Universität Frankfurt am Main, Frankfurt, Germany. *email: hosanna@anu.ac.kr

Ca^{2+} level[28]. Besides, 5-HT_4, 5-HT_6, and 5-HT_7 receptors coupled to G_s can stimulate cAMP production[28]. However, 5-HT_3 receptor is a ligand-gated cation channel that mediates neuronal depolarization[29].

Insects have at least three subtypes of 5-HT receptors. Five different 5-HT receptors as orthologous to mammalian 5-HT_{1A}, 5-HT_{1B}, 5-HT_{2A}, 5-HT_{2B}, and 5-HT_7 have been identified in *D. melanogaster*[14]. In addition, partial sequences of two 5-HT_1, two 5-HT_2, and one 5-HT_7 receptors have been identified in the field cricket *Gryllus bimaculatus*[30]. Two 5-HT_1 receptors and two 5-HT_1 splice variants have been described in *Tribolium castaneum* and *Papilio xuthus*, respectively[31,32]. As from *D. melanogaster* and *G. bimaculatus*, two 5-HT_2 receptors have been described from *Apis mellifera* while only one 5-HT_2 receptor has been reported in other insects such as *Periplaneta americana* and *Locusta migratoria*3[33,34]. In a lepidopteran species, *Pieris rapae*, four different 5-HT receptors including a novel subtype 8 have been reported[35,36].

5-HT modulates various physiological processes via expression of different receptor types in various tissues. 5-HT receptors are expressed highly in brain and ventral nerve cord of insects[32]. 5-HT_1 receptor in honey bee brain is involved in visual information processing[37]. Expression pattern of 5-HT_7 receptor in honey bee nervous system suggests its possible roles in information processing, learning, and memory[38]. 5-HT receptors might play roles in neuroendocrine secretion and gut motility in cockroaches[29]. In salivary gland of several insects, 5-HT_7 receptor has been reported to be involved in salivary secretion mediated by cAMP level elevation[33,39,40]. Moreover, 5-HT_7 receptor mediates visceral muscle contraction in the gastrointestinal tract of several insects including *A. aegypti* and *T. castaneum*[41,42]. 5-HT not only has neurophysiological roles, but also mediates cellular immune responses in insects by enhancing phagocytosis and nodulation[43]. Two different 5-HT receptors (1B and 2B) are expressed in hemocytes of *P. rapae*, of which 5-HT receptor 1B mediates cellular immune response[22]. In another lepidopteran insect, *Spodoptera exigua*, 5-HT mediates increase of total circulatory hemocyte number by stimulating sessile hemocytes and mediating cellular immune responses such as phagocytosis and nodule formation[44,45]. However, 5-HT receptor in *S. exigua* has not been reported yet.

Two entomopathogenic bacteria, *Xenorhabdus* and *Photorhabdus*, can inhibit insect immune responses to protect themselves and their symbiotic nematodes[46]. To accomplish host immunosuppression, these bacteria can synthesize and secrete secondary metabolites to inhibit immune signals and effectors[47]. Among these bacterial metabolites, tryptamine and phenylethylamide derivatives have been identified with suggested function of interrupting 5-HT signaling[48]. The objective of the present study was to determine bacterial secondary compound(s) that could inhibit 5-HT signaling. To this end, we identified 5-HT receptor that could mediate insect immunity in *S. exigua*. To determine a potent inhibitor of this receptor, we screened bacterial secondary metabolites and their potent derivatives.

Results

Bioinformatics analyses reveal that *S. exigua* contains a 5-HT receptor. From a short read archive database (GenBank accession number: SRR1050532) of *S. exigua*, a highly matched contig (accession number: GARL01017386.1) containing 3,308 bp nucleotide sequence with an open reading frame (ORF) from 996th to 2,690th bp was identified. Prediction of amino acid sequence by BlastP analysis revealed that its ORF sequence shared identities with other insect 5-HT receptors: 99% with *Spodoptera litura* 5HTR (XP_022827337.1), 98% with *Helicoverpa armigera* 5HTR (XP_021195909.1), 95% with *Trichoplusia ni* 5HTR (XP_026729862.1), and 85% with *Manduca sexta* 5HTR (AGL46976.1). This novel 5-HT receptor from *S. exigua* (Se-5HTR) encoded a sequence of 564 amino acids having a predicted molecular weight of about 63.23 kDa. Phylogenetic analysis of its protein sequence indicated that Se-5HTR was clustered with other 5-HT_7 receptors (Fig. 1a). Predicted amino acid sequence of Se-5HTR contained a signal peptide of 35 residues and attained GPCR character with seven transmembrane domains. Consensus N-linked glycosylation sites are located in the N-terminus (Asn48 and Asn53), the third intracellular loop (Asn362), and C-terminus (Asn534). Several consensus sites for phosphorylation by protein kinase A and/or protein kinase C were predicted throughout the length of the sequence. A disulfide bond between two Cys residues at extracellular matrix ('ECM', Supplementary Fig. 1) is also predicted.

Se-5HTR sequence attains highly conserved amino acid residues (Fig. 1b) found uniquely in the biogenic monoamine receptor family[49–51]. Negatively charged Asp residue in TM3 (Asp163) might interact with positively charged amino group of the ligand. A hydrogen bond between the hydroxyl group of serine residue in TM5 (Ser247) and the hydroxyl group of 5-HT was predicted. In TM6, the consensus sequence unique to aminergic receptors (Phe444-X-X-X-Trp448-X-Pro450-X-Phe452) is conserved. Like other GPCRs, a possible motif (Asn485-Pro486-X-X-Tyr489) that might participate in agonist-mediated sequestration and re-sensitization of Se-5HTR is conserved in TM7. The C-terminus of the receptor contains two potential post-translational palmitoylation cysteine residues (Cys508 and Cys-532) and PDZ (post synaptic density protein, *Drosophila* disc large tumor suppressor, and zonula occludens-1 protein)-domain binding motif (Glu561-Ser562-Phe563-Leu564).

Se-5HTR is expressed in all developmental stages and larval tissues. Expression of *Se-5HTR* in different developmental stages of *S. exigua* was assessed by RT-PCR. Results showed its expression from egg to adult stages (Fig. 2a). RT-qPCR revealed variation in its expression among developmental stages, with L5 larvae and adults showing the highest expression levels. In L5 larvae, all tissues analyzed by RT-PCR showed its expression (Fig. 2b). RT-qPCR revealed that the midgut exhibited the highest expression level of *Se-5HTR*. Hemocytes and brain also showed relatively high levels of its expression. Basal expression levels of *Se-5HTR* were highly up-regulated in response to immune challenge (Fig. 2c). *Se-5HTR* expression was increased ~125-fold after challenge with fungus, *Beauveria bassiana* compared to control (unchallenged). It was increased 60~90-fold after bacterial challenge compared to naïve larvae.

Specific inhibitors against 5-HTR suppress hemocyte behaviors of *S. exigua*. A commercial inhibitor (SB-269970) specific to 5-HT_7 was used to assess its effect on hemocyte behaviors of *S. exigua* (Fig. 3).

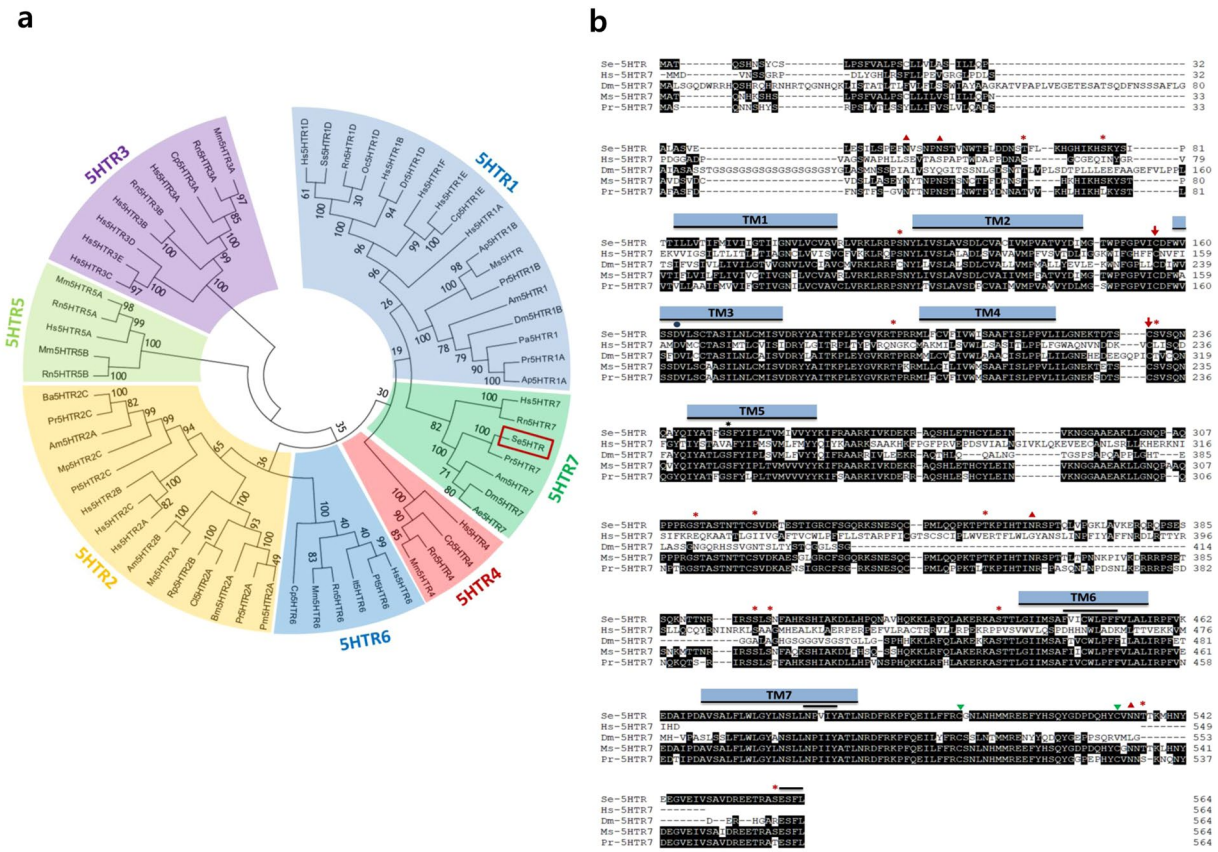

Figure 1. Bioinformatics analysis of a novel 5-HTR$_7$ identified from *S. exigua* (Se-5HTR: MH025798). (**a**) Phylogenetic analysis of 5HTRs. Amino acid sequences were retrieved from GenBank: Hs5HTR1D (NP_000855.1), Ss5HTR1D (NP_999323.1), Rn5HTR1D (NP_036984.1), Oc5HTR1D (NP_001164624.1), NP_000854.1 Hs5HTR1B (NP_000854.1), Dr5HTR1D (NP_001139158.1), Hs5HTR1F (NP_000857.1), Hs5HTR1E (NP_000856.1), Cp5HTR1E (NP_001166222.1), Hs5HTR1A (NP_000515.2), Ap5HTR1B (ABY85411.1), Ms5HTR (ABI33827.1), Pr5HTR1B (XP_022120028.1), Am5HTR1 (NP_001164579.1), Dm5HTR1B (NP_001163201.2), Pa5HTR1 (CAX65666.1), Pr5HTR1A (XP_022129638.1), Ap5HTR1A (ABY85410.1), Hs5HTR7 (P34969), Rn5HTR7 (P32305), Pr5HTR7 (AMQ67549.1), Am5HTR7 (NP_001071289.1), Dm5HTR7 (NP_524599.1), Ae5HTR7 (Q9GQ54), Hs5HTR4 (Q13639), Cp5HTR4 (O70528), Rn5HTR4 (Q62758), Mm5HTR4 (P97288), Hs5HTR6 (P50406), Pt5HTR6 (Q5IS65), It5HTR6 (XP_005317590.1), Rn5HTR6 (P31388), Mm5HTR6 (Q9R1C8), Cp5HTR6 (XP_003471412.1), Pm5HTR2A (KPJ17794.1), Pr5HTR2A (XP_022112310.1), Bm5HTR2A (NP_001296483.1), Cl5HTR2A (XP_014254278.1), Rp5HTr2B (AKQ13312.1), Mq5HTR2A (KOX78271.1), Am5HTr2B (NP_001189389.1), Hs5HTR2A (NP_000612.1), Hs5HTR2C (NP_000859.1), Hs5HTR2B (NP_000858.3), Pt5HTR2C (XP_015921531.1), Mp5HTR2C (XP_022169104.1), Am5HTr2A (NP_001191178.1), Pr5HTR2C (XP_022122944.1), Ba5HTR2C (XP_023955125.1), Rn5HTR5B (P35365), Mm5HTR5B (P31387), Hs5HTR5A (NP_076917.1), Rn5HTR5A (P35364), Mm5HTR5A (P30966), Hs5HTR3C (NP_570126.2), Hs5HTR3E (NP_001243542.1), Hs5HTR3D (NP_001157118.1), Hs5HTR3B (NP_006019.1), Rn5HTR3B (NP_071525.1), Hs5HTR3A (AP35868.1), Cp5HTR3A (O70212), Rn5HTR3A (NP_077370.2), Mm5HTR3A (P23979). The phylogenetic tree was constructed using neighbor-joining method. Bootstrap values on branch nodes were obtained after 1,000 repetitions. (**b**) Amino acid sequence alignment of Se-5HTR with orthologous receptors from *Homo sapiens* (Hs-5HTR7: P34969), *Drosophila melanogaster* (Dm-5HTR7: NP_524599.1), *Manduca sexta* (Ms-5HTR7: AGL46976.1), and *Pieris rapae* (Pr-5HTR7: AMQ67549.1). Identical residues among these five sequences are illustrated as white letters against black. Dashes within sequences indicate gaps introduced to maximize homology. Putative seven transmembrane domains (TM1-TM7) are shown as blue bars. Potential N-glycosylation sites (red triangle), potential phosphorylation sites for protein kinase A and/or C (red asterisk), potential residue to interacts with 5-HT amino group (black closed circle) and 5-HT hydroxyl group (black asterisk), potential disulfide bond groups (red down arrow), and potential post translational palmitoylation sites (green triangle) are indicated. Overbars indicate unique motif to aminergic receptor, agonist mediated sequestration and resensitization motif, and PDZ-domain binding motif, respectively. Conserved domains were determined using InterPro tool (https://www.ebi.ac.uk/interpro/) and Prosite (http://prosite.expasy.org/) whereas other residues and motifs were predicted using several tools from DTU bioinformatics (www.cbs.dtu.dk/services/).

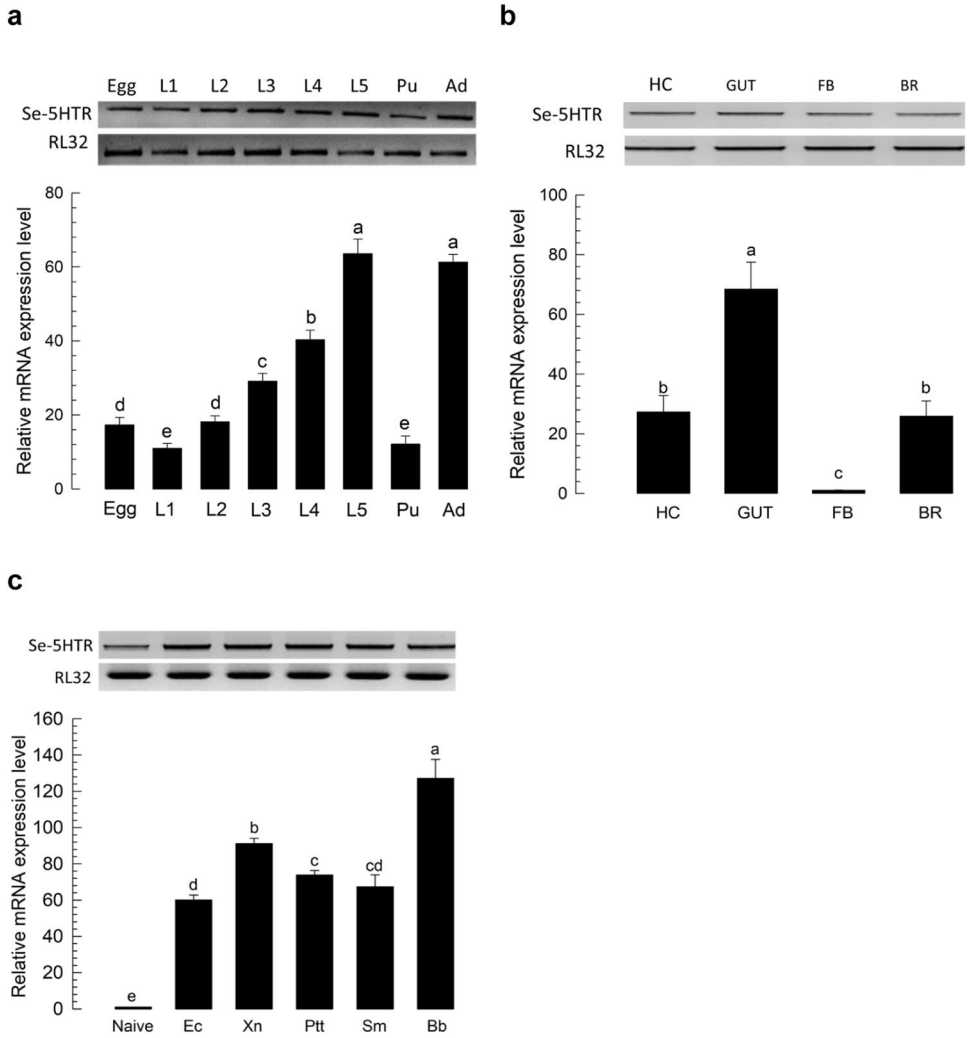

Figure 2. Expression profile of *Se-5HTR*. (**a**) Differential expression of *Se-5HTR* in different developmental stages: egg, larval instars ('L1-L5'), pupa ('Pu'), and adult ('Ad'). (**b**) Differential expression of *Se-5HTR* in different tissues of L5 larvae: hemocyte ('HC), midgut ('GUT'), fat body ('FB'), and brain ('BR'). (**c**) Expression pattern of *Se-5HTR* in immune-challenged L5 larvae: *Escherichia coli* ('Ec'), *Xenorhabdus nematophila* ('Xn'), *Photorhabdus temperata temperata* ('Ptt'), *Serratia marcescens* ('Sm'), and *Beauveria bassiana* ('Bb'). Immune challenge was performed by injecting each L5 larva with 1.8×10^5 cells of bacteria or 5×10^5 conidia of fungi. After incubation at 25 °C for 8 h, gene expression analysis was performed using RT-PCR and RT-qPCR. As a constitutive expressional control, a ribosomal gene, *RL32*, was used for expression analysis in RT-PCR and RT-qPCR. Each measurement was replicated three times with independent biological samples. Histogram bars annotated with the same letter are not significantly different at Type I error = 0.05 (LSD test).

Total hemocyte count (THC) of L5 larvae was ~1.2×10^7 cells/mL (Fig. 3a). THC was significantly ($P < 0.05$) increased in response to 5-HT or bacterial challenge. SB-269970 prevented the increase of THC in response to bacterial challenge. Its IC_{50} value was estimated to be 1.925 μM. These results suggest that Se-5HTR can mediate hemocyte mobilization in response to 5-HT upon bacterial challenge.

To determine the modulation effect of Se-5HTR on hemocyte-spreading behavior, competitive inhibition between SB-269970 and 5-HT against Se-5HTR was assessed (Fig. 3b). Hemocytes were spread on slide glass with growth of F-actin. However, SB-269970 significantly ($P < 0.05$) suppressed such hemocyte-spreading behavior. The inhibitory effect of the inhibitor was rescued by addition of 5-HT. A relatively low dose (SB-269970: 5-HT = 10:1) of 5-HT did not rescue the inhibitory effect. However, a relatively high dose (1:10) of 5-HT significantly ($P < 0.05$) rescued such inhibitory effect, indicating a specific competition between inhibitor and ligand against Se-5HTR.

RNA interference (RNAi) of Se-5HTR. To address the immunomodulatory effect of Se-5HTR on hemocytes, its gene expression was knocked-down by RNAi (Fig. 4). RNAi was performed using dsRNA specific to *Se-5HTR*. dsRNA-injected larvae exhibited significant ($P < 0.05$) reduction of *Se-5HTR* expression. RT-qPCR analysis showed that about 90% of *Se-5HTR* mRNA was suppressed by dsRNA treatment at 24 h PI (Fig. 4a). At

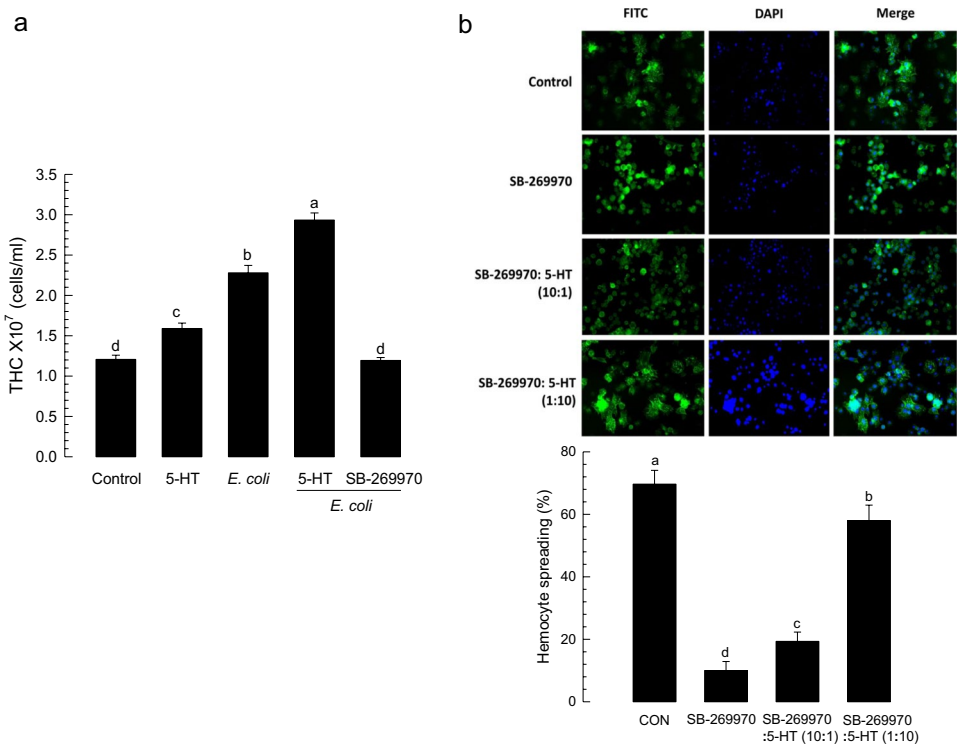

Figure 3. Effect of an inhibitor specific to 5-HT_7 receptor ('SB-269970') on hemocyte behaviors of *S. exigua*. (**a**) Total hemocyte count (THC) analysis in L5 larvae. For the assay, 2 µg of 5-HT or 2 µg of SB-269970 was injected. THC was assessed with or without bacterial co-injection (1.8×10^5 cells per larva). (**b**) Hemocyte-spreading behavior analysis. Hemocyte-spreading was assessed with a 20 µL reaction mixture containing 1 or 2 µL test chemical with 18 or 19 µL hemocytes. 5-HT was co-applied with SB-269970 at ratios of 1:10 (2 µg 5-HT: 20 µg SB-269970) and 10:1 (20 µg 5-HT: 2 µg SB-269970). Spread cells were stained with F-actin and FITC-labeled phalloidin. Nuclei were stained with DAPI. Each treatment was independently replicated three times. Histogram bars indicate percentages of spread hemocytes and error bars indicate standard deviation. Histogram bars annotated with the same letter are not significantly different at Type I error = 0.05 (LSD test).

24 h PI of dsRNA, *Se-5HTR* expression was analyzed in four different tissue samples. Compared to control tissues, dsRNA-treated larvae exhibited significant ($P < 0.05$) reduction of *Se-5HTR* expression in all tissues including hemocytes.

RNAi of Se-5HTR suppresses hemocyte behaviors of *S. exigua*. The effect of RNAi specific to Se-5HTR on hemocyte mobilization in response to bacterial challenge was analyzed (Fig. 4b). Upon bacterial challenge, THC increased by more than two folds. However, RNAi treatment significantly ($P < 0.05$) suppressed such increase of THC. The RNAi treatment also significantly ($P < 0.05$) influenced hemocyte-spreading behavior (Fig. 4c). On glass slide, hemocytes exhibited spreading behavior in 40 min by cytoskeletal rearrangement through F-actin growth (see phalloidin staining). However, hemocytes collected from larvae treated with RNAi specific to Se-5HTR lost such behavior.

Modulation of cellular immune responses by Se-5HTR. The influence of Se-5HTR on modulating hemocyte-spreading behavior suggested that it might mediate cellular immune responses against bacterial infection. Phagocytosis against FITC-labeled *Escherichia coli* was observed in hemocytes from control larvae. Labeled bacteria were observed within hemocytes of control larvae (Fig. 5a). However, hemocytes of larvae treated with dsRNA specific to Se-5HTR significantly ($P < 0.05$) lost such phagocytosis, similar to that found for hemocytes of larvae treated with SB-269970. Phagocytosis was decreased around 57% or 78% after treatment with dsRNA or inhibitor, respectively. In response to bacterial challenge, *S. exigua* formed ~78 hemocytic nodules per larva (Fig. 5b). However, RNAi specific to Se-5HTR or inhibitor treatment significantly ($P < 0.05$) reduced such cellular immune response.

CRISPR-Cas9 of *Se-5HTR* and its influence on phagocytosis. To support the function of Se-5HTR in mediating cellular immunity, a CRISPR-Cas9-mediated knockout of *Se5HTR* was performed (Fig. 6). In *in vitro* test, the designed sgRNA was able to specifically bind to target DNA (638 bp, Fig. 6a) and mediated DNA cleavage by Cas9 (Fig. 6b). The sgRNA and Cas9 enzyme complex was injected to newly laid eggs. Control (Cas9 only) injection (n = 300) showed 66.3% of hatching ration while treatment (sgRNA + Cas9) injection (n = 800) showed 12.1%. Among hatched larvae, 94.4% larvae developed to pupae in control compared to 15.4% in treatment. At L5 larvae, the mutant larvae were assessed in their genomic DNA sequences at the target region and showed deletions compared to control larvae (Fig. 6c). The deletion mutations led to missense and partial deletion in amino

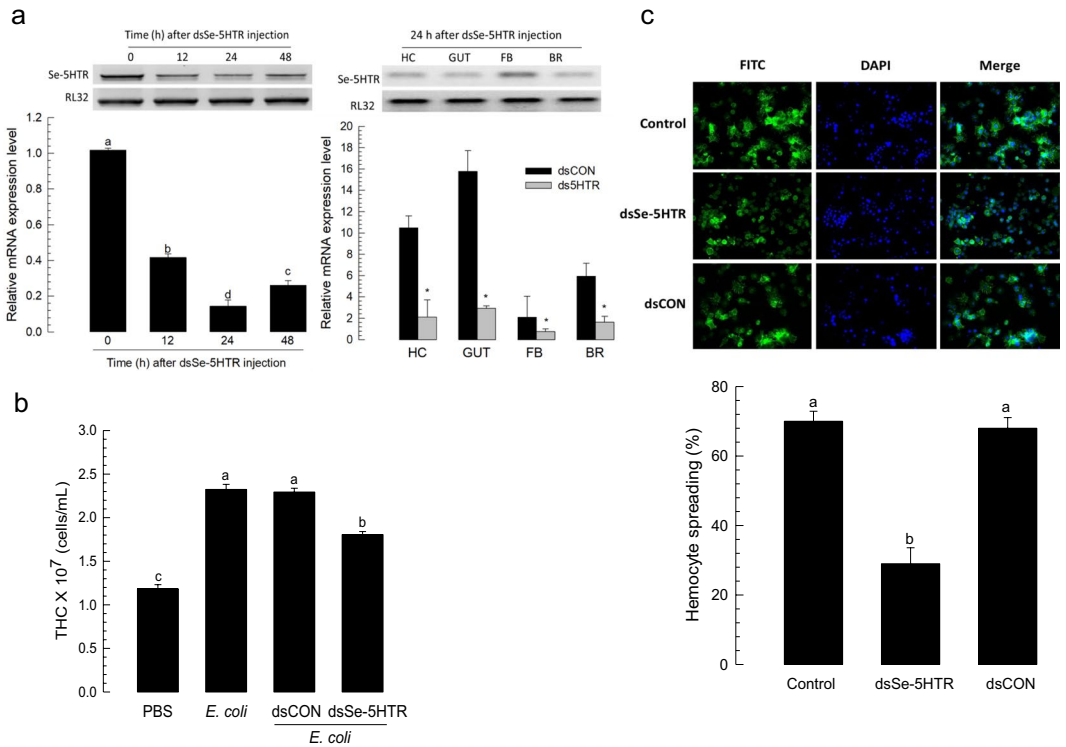

Figure 4. RNA interference (RNAi) of *Se-5HTR* and suppression of hemocyte behaviors. (**a**) RNAi of *Se-5HTR* expression with a gene-specific dsRNA (dsSe-5HTR). About 900 ng of dsSe-5HTR was injected to L5. At 0, 12, 24, and 48 h post-injection (PI), expression levels of *Se-5HTR* were assessed from whole body. Expression levels of *Se-5HTR* in different tissue parts were assessed at 24 h PI. As a constitutive expressional control, a ribosomal gene, *RL32*, was used for expression analysis in RT-PCR and RT-qPCR. As a control RNAi (dsCON), dsRNA specific to *CpBV-ORF302* (a viral gene) was used for expression analysis. In RT-qPCR, each treatment was triplicated. (**b**) Influence of RNAi on up-regulation of total hemocyte count (THC) in response to bacterial challenge. At 24 h PI of dsSe-5HTR, hemolymph was collected from L5 larvae for THC assessment. Each treatment was replicated three times. (**c**) Influence of RNAi on hemocyte-spreading behavior. For spreading assay, hemocytes from larvae treated with dsRNA were collected at 24 h. Each treatment was independently replicated three times. Spread cells were stained with F-actin and FITC-labeled phalloidin. Nuclei were stained with DAPI. Histogram bars indicate percentages of spread hemocytes and error bars indicate standard deviation. Different letters above standard error bars indicate significant difference among means at type I error = 0.05 (LSD test). Asterisks represent significant difference between control and treatment in each tissue.

acid sequence ('M2') or early termination in other mutants. Under this knockout condition, mutant larvae were assessed in cellular immune response using phagocytosis (Fig. 6d). Control larvae enhanced the phagocytotic activity with addition of 5-HT. However, knockout mutants were significantly impaired in the immune response, in which the enhancement of the phagocytotic activity in response to 5-HT was lost.

Influence of bacterial secondary metabolites on immune responses mediated by Se-5HTR. RNAi or specific inhibitor assays indicated that 5-HTR could mediate both cellular immune responses of phagocytosis and nodule formation in response to bacterial challenge. Bacterial metabolites of two entomopathogens, *Xenorhabdus nematophila* (Xn) and *Photorhabdus temperata temperata* (Ptt), were extracted from their culture broth using different organic solvents and their inhibitory activities against cellular immune responses were then assessed (Fig. 7). Organic solvent extracts of Xn- or Ptt-cultured broth exhibited significant ($P < 0.05$) inhibitory activities against phagocytosis (Fig. 7a) and nodulation (Fig. 7b), although there were variations in their inhibitory activities among extracts.

To identify bacterial secondary compounds that could inhibit Se-5HTR, 37 compounds (HB 4 – HB 602) derived from *Xenorhabdus* and *Photorhabdus*[47] were screened for their inhibitory activities against hemocyte nodule formation and phagocytosis (Fig. 8). More than three 75% (28 out of 37 compounds) of these test compounds exhibited significant ($P < 0.05$) inhibition against phagocytosis (Fig. 8a). In nodulation assay, all test compounds exhibited significant ($P < 0.05$) inhibition (Fig. 8b). Since Se-5HTR could mediate both cellular immune responses, bacterial compounds that highly inhibited both phagocytosis (<60%) and nodulation (<30 nodules per larva) were selected. As a result, 10 potent chemicals (HB 4, HB 5, HB 23, HB 30, HB 44, HB 45, HB 50, HB 223, HB 302, and HB 531) belonging to six chemical categories [phenylethylamide (PEA), tryptamide, xenortide, xenocycloin, nematophin, and GameXPeptide] were found (Supplementary Fig. 2). All these compounds exhibited median inhibitory concentration (IC_{50}) of 58∼253 μM against cellular immune response of hemocytic nodulation.

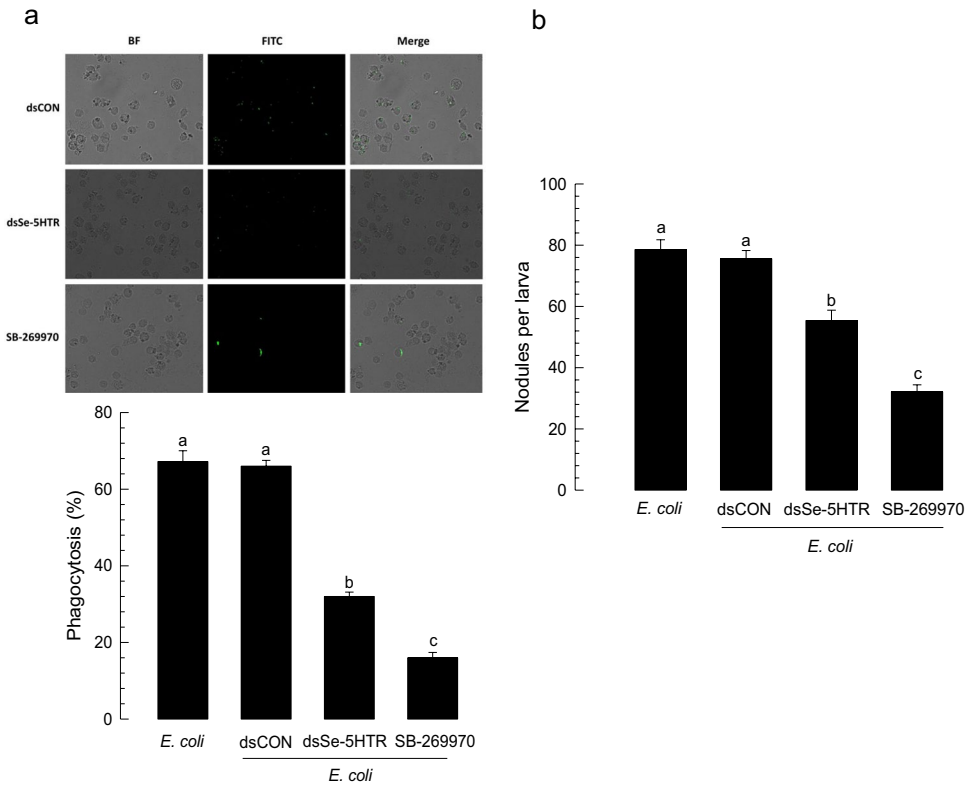

Figure 5. RNA interference (RNAi) of *Se-5HTR* and suppression of cellular immune responses. (**a**) Analysis of phagocytosis in L5 larvae of *S. exigua*. FITC-tagged *E. coli* were injected into L5 larvae at 24 h post-injection of dsSe-5HTR. A specific inhibitor (SB-269970) to 5-HT_7 receptor was co-injected at a dose of 2 µg along with FITC-tagged bacteria. At 15 min after injection, phagocytic cells were observed under a fluorescent microscope at 400 × magnification and percentage of phagocytotic hemocytes was calculated from randomly chosen 100 cells. Total hemocytes were observed from bright-field ('BF'). Each treatment was independently replicated three times. (**b**) Nodulation assay. After RNAi, *E. coli* (1.8×10^5 cells/larva) was injected to L5 larvae. SB-269970 (2 µg/larva) was co-injected with bacteria. After 8 h incubation at 25 °C, treated insects were assessed for nodule formation. Histogram bars indicate percentages of phagocytosis and error bars indicate standard deviation. Histogram bars annotated with the same letter are not significantly different at Type I error = 0.05 (LSD test).

To support the specific inhibitory activity of these selected compounds against Se-5HTR, competitive assay was performed between test compounds and 5-HT (Fig. 9). With a constant concentration of 5-HT, phagocytic behavior of *S. exigua* hemocytes gradually decreased with increasing amount of test compound (Fig. 9a). On the other hand, increase of 5-HT amount gradually decreased the phagocytotic behavior using a constant amount of test compound (Fig. 9b).

Influence of PEA derivatives on phagocytosis mediated by Se-5HTR. These 10 selected compounds shared phenyl (or aromatic) ethylamide backbone except xenocycloin (Supplementary Fig. 2). Based on PEA backbone, 45 derivatives were selected from a chemical bank and their inhibitory activities against the phagocytotic behavior of *S. exigua* hemocytes were tested (Fig. 10a). More than 66% (30 out of 45 compounds) of PEA derivatives exhibited significant ($P < 0.05$) inhibition against phagocytosis. Three PEA derivatives (Ph15, Ph17, Ph33) had inhibitory activities similar to a bacterial metabolite (HB 44), with IC_{50} at 1.8 ∼ 5.6 µM against phagocytosis (Fig. 10b). These three PEA derivatives competitively inhibited the phagocytosis mediated by Se-5HTR (Fig. 10c).

Synthesis of a potent inhibitor and inhibitory efficacy against Se-5HTR. Potent compounds from 45 PEA derivatives were analyzed for their structures and activities against phagocytosis mediated by Se-5HTR (Supplementary Fig. 3). They shared the PEA backbone. However, they had different side chains at 'X' and 'Y' (Supplementary Fig. 3a). When different X substituents were compared for their inhibitory activities, methoxy was the most potent moiety (Supplementary Fig. 3b). When different Y substituents were compared for their inhibitory activities with respect to identical X groups, hexahydropyrrolo[1,2-a]pyrazine-1,4-dione was the most potent moiety (Supplementary Fig. 3c). This analysis allowed us to design a hypothetical compound containing methoxy in X and hexahydropyrrolo[1,2-a]pyrazine-1,4-dione at Y based on PEA backbone (Supplementary Fig. 3d).

The designed compound ('PhX') was chemically synthesized and in its inhibitory activity against phagocytosis was assessed compared with a specific 5-HT_7 inhibitor, SB269970, as a reference (Fig. 11). PhX was highly potent. It competitively inhibited cellular immune response with 5-HT. Its inhibitory activity was more potent ($t = 14.9$; df = 32; $P < 0.0001$) than SB269970.

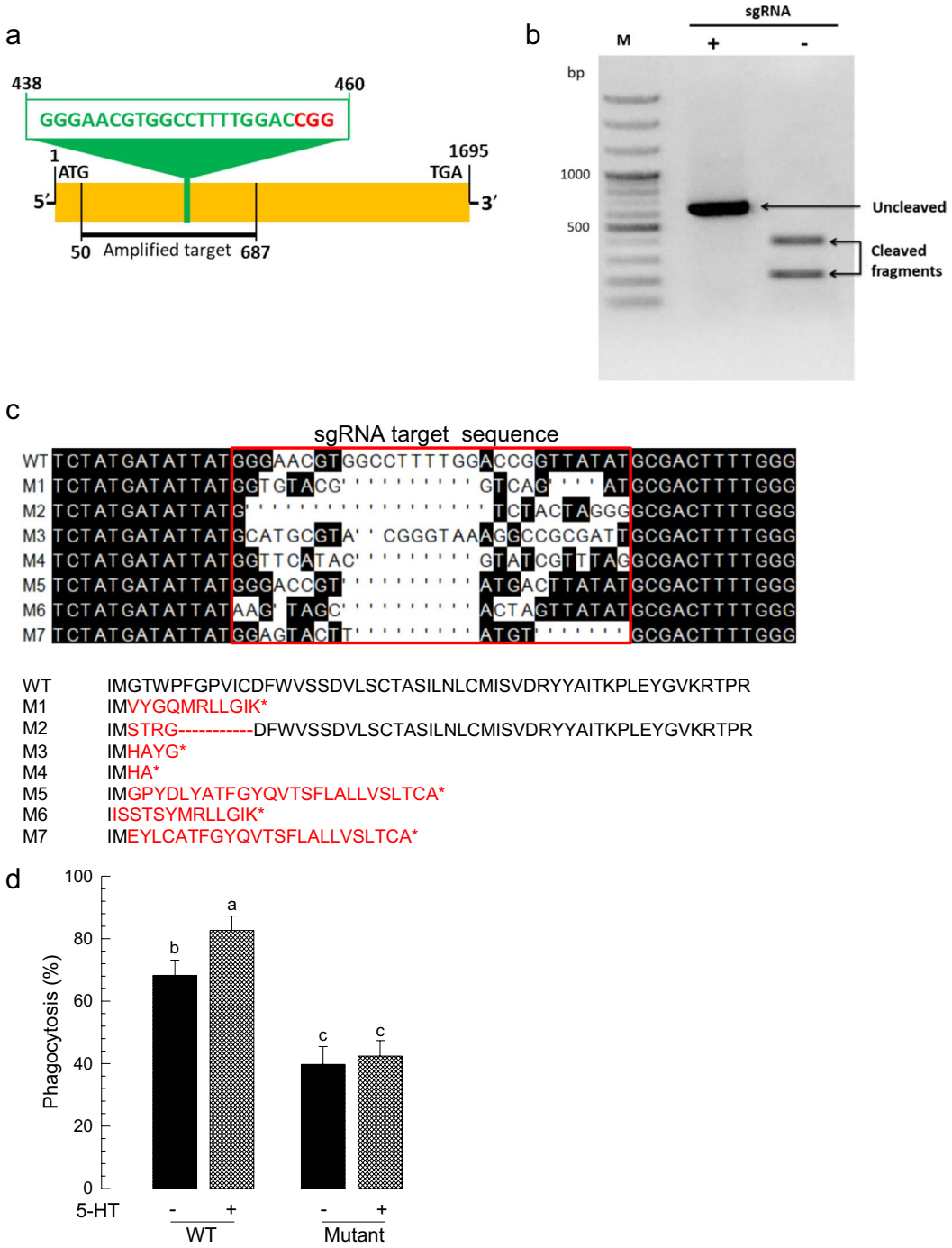

Figure 6. Knockout mutant of *S. exigua* in *Se-5HTR* using CRISPR-Cas9 and its insensitivity to 5-HT. (**a**) Schematic representation of single-stranded guide RNA (sgRNA) target site on Se-5HTR. The target sequence is shown in green color with the protospacer adjacent motif (PAM) in red color. (**b**) *In vitro* test of sgRNA specificity. Target DNA fragment (638 bp) was amplified. Reaction mixture (15 uL) consisted of target DNA (250 ng), sgRNA (50 ng), and Cas9 (250 ng). (**c**) Mutation in target sites after CRISPR-Cas9. Late instar larvae were bled to collect hemocytes, from which genomic DNA was extracted for sequencing analysis. Seven mutants (M1-M7) are compared with control (WT) in the DNA region. Deduced amino acid sequences in the target region are compared among WT and mutants, in which asterisk indicates early termination. (**d**) Insensitivity of knockout mutants to 5-HT with respect to phagocytosis. Hemocyte was collected from test larvae and used for *in vitro* phagocytosis assay with 5-HT (940 μM). All treatments were replicated three times. Different letters above standard deviation bars represent significant difference among means at Type I error = 0.05 (LSD test).

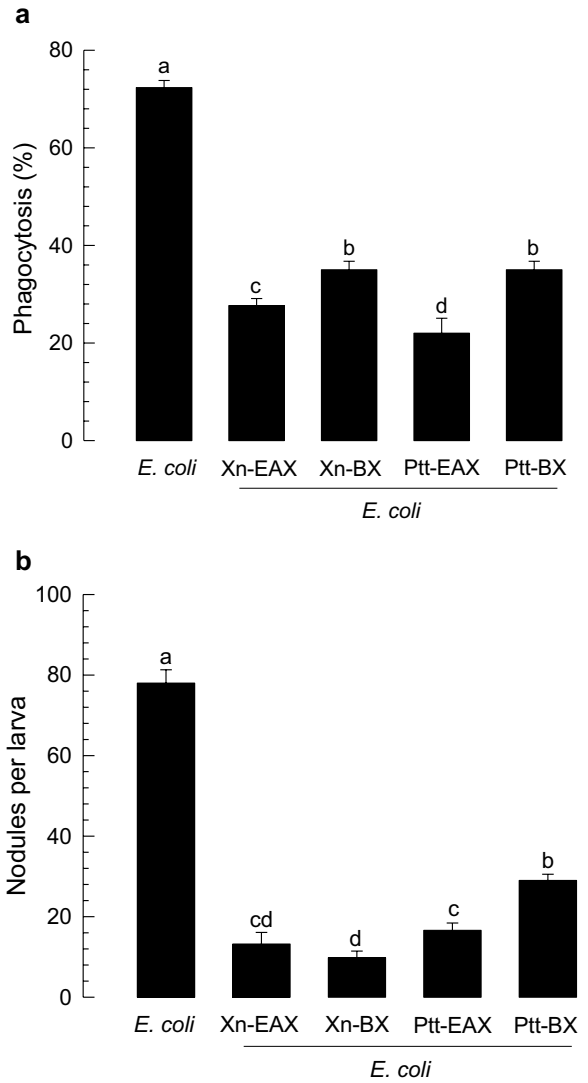

Figure 7. Immunosuppressive activities of organic extracts from culture broth of *Xenorhabdus nematophila* ('Xn') and *Photorhabdus temperata temperata* ('Ptt') bacteria against L5 larvae of *S. exigua*. Each larva was injected with *E. coli* (10^5 cells) along with 1 μL of ethyl acetate ('EAX') or butanol ('BX') extract. (**a**) Phagocytosis in L5 larvae. FITC-tagged *E. coli* were injected to L5 larvae at 24 h post-injection of an organic extract. After 15 min, phagocytic cells were observed under a fluorescent microscope at 400 × magnification and percentage of phagocytotic hemocytes was calculated from randomly chosen 100 cells. Each treatment was independently replicated three times. (**b**) Nodule formation. *E. coli* (1.8×10^5 cells/larva) was injected to L5 larvae. An organic extract was co-injected with the bacteria. After 8 h of incubation at 25 °C, treated insects were assessed for nodule formation. Each treatment was replicated with 10 larvae. Different letters above standard deviation bars indicate significant difference among means at Type I error = 0.05 (LSD test).

Discussion

5-HT plays a crucial role in mediating cellular immune responses of *S. exigua* by stimulating actin rearrangement[45]. Furthermore, it performs a functional cross-talk with eicosanoid signaling via a small G protein Rac1[52]. However, its signaling pathway leading to immune responses remains unclear due to the lack of its receptor information in *S. exigua*. This study identified a 5-HT receptor and showed its physiological function in mediating immune responses.

Se-5HTR attains seven transmembrane domains and shares common molecular characters with other 5-HT receptors. Like other GPCRs, Se-5HTR contains the canonical seven transmembrane domains along with consensus glycosylation in the N-terminus (Asn48 and Asn53)[53]. Additionally, its sequence contains a consensus aspartic acid residue in TM3 (Asp163) and a serine residue in TM5 (Ser247) to interact with functional groups of biogenic monoamines[54]. At the intracellular border of TM3, the highly conserved Asp180-Arg181-Tyr182 motif is evident for a strong ionic interaction with Glu430 residue adjacent to the intracellular end of TM6 that plays a crucial role in GPCR signal transduction[55]. The sequence contains consensus Phe444-X-X-X-Trp448-X-Pro4 50-X-Phe452 motif in TM6 which is unique to biogenic monoamine GPCRs[38]. Additionally, Se-HTR contains

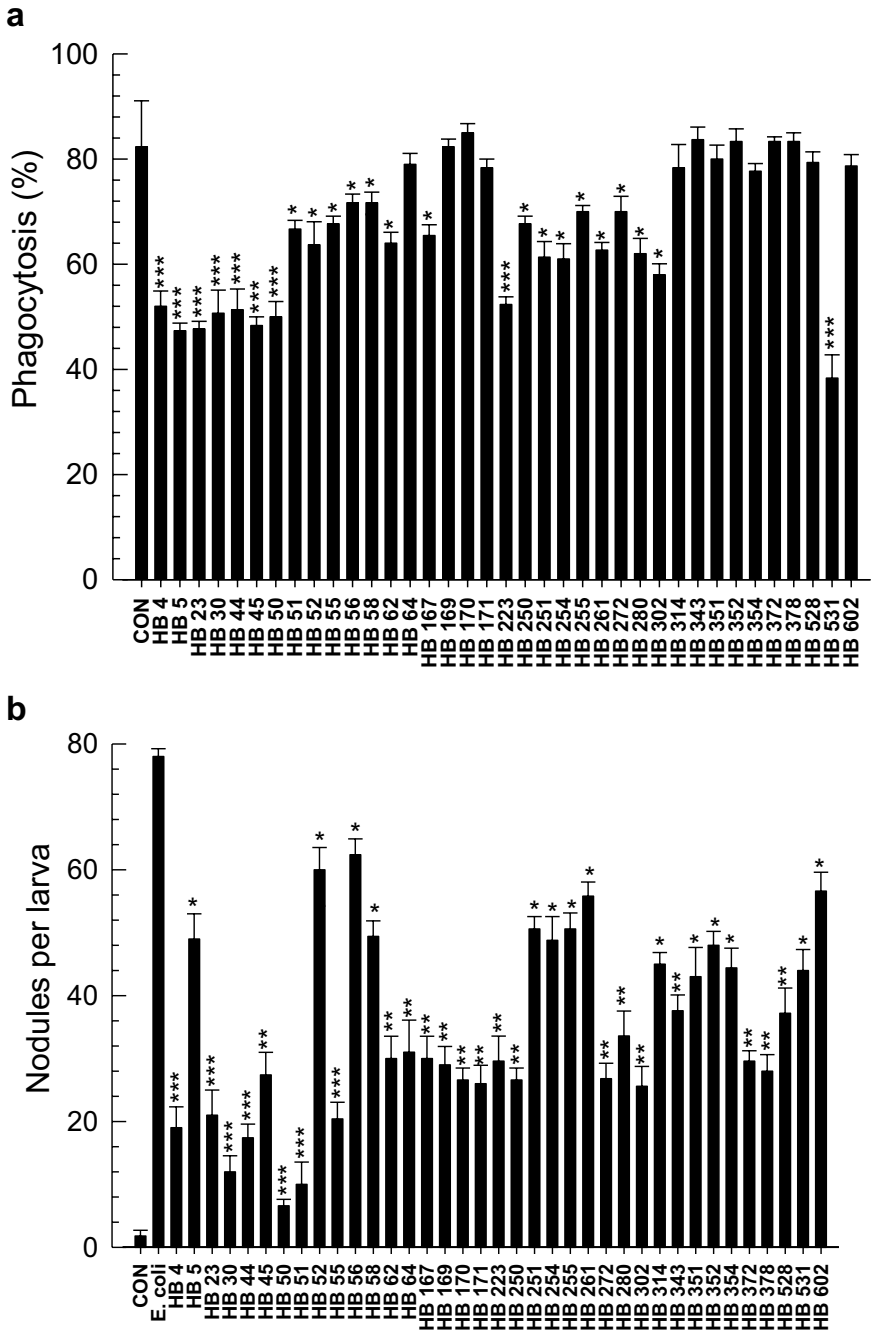

Figure 8. Screening 37 bacterial secondary metabolites derived from *X. nematophila* and *P. temperata temperata* for their effects on cellular immune responses mediated by Se-5HTR in *S. exigua*. (**a**) Screening with phagocytosis assay. FITC-tagged *E. coli* cells were injected to L5 larvae along with 1 μg of each test chemical. After 15 min, phagocytic cells were observed under a fluorescent microscope at 400 × magnification and percentage of phagocytotic hemocytes was calculated from randomly chosen 100 cells. Each treatment was independently replicated three times. (**b**) Screening with nodule formation assay. *E. coli* (1.8×10^5 cells/larva) was injected to L5 larvae along with 1 μg of each test chemical. After 8 h of incubation at 25 °C, treated insects were assessed for nodule formation. Each treatment was replicated with 10 larvae. Asterisks above standard deviation bars indicate significant difference compared to control ('CON' without inhibitor) at Type I error = 0.05 (*), 0.01 (**), and 0.005 (***) (LSD test).

two potential post-translational palmitoylation cysteine residues (Cys508 and Cys532)[56] at the final intracellular region with a PDZ-domain binding motif (Glu561-Ser562-Phe563-Leu564) at the C-terminus[57].

Se-5HTR is expressed in all developmental stages. It is expressed in immune-associated tissues (hemocytes and fat body), digestive (gut) tissues, and nervous (brain) tissues at larval stage. Three 5-HT receptors of *P. rapae*

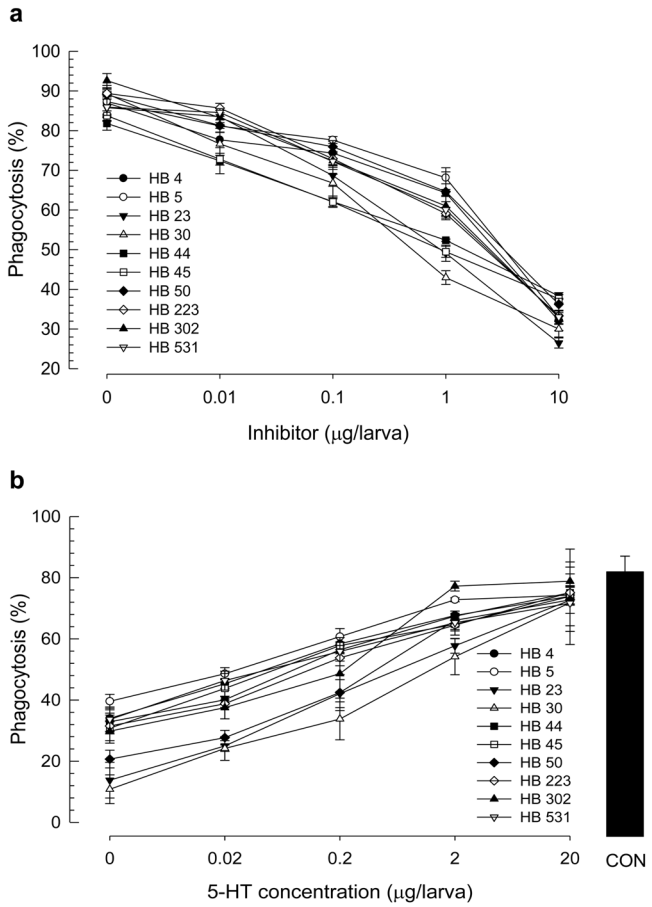

Figure 9. Competitive inhibition of 10 selected bacterial metabolites derived from *X. nematophila* and *P. temperata temperata* with 5-HT against Se-5HTR mediating phagocytosis. FITC-tagged *E. coli* cells were injected to L5 larvae along with test chemicals. After 15 min, phagocytic cells were observed under a fluorescent microscope at 400 × magnification and percentage of phagocytotic hemocytes was calculated from randomly chosen 100 cells. Each treatment was independently replicated three times. (**a**) Dose-response of inhibitory compound (0, 0.01, 0.1, 1, and 10 μg/larva) with a fixed 5-HT concentration (1 μg/larva). (**b**) Dose-response of 5-HT (0, 0.02, 0.2, 2 and 20 μg/larva) with a fixed HB compound concentration (1 μg/larva). 'CON' represents a positive control without any inhibitor.

larvae are all expressed, although their expression levels in tissues are different. Subtypes 1A and 1B receptor are highly expressed in nervous tissues while subtype 7 receptor is mainly expressed in digestive tissue[36]. *Se-5HTR* was also highly expressed in the gut like 5-HT_7 of *P. rapae*. Furthermore, our phylogenetic analysis of 5-HT receptors showed that these two insect 5-HT_7s were closely related and clustered. Expression levels of *Se-5HTR* in hemocytes were similar to those in the brain. This suggests that Se-5HTR is associated with immune function as well as neurophysiological function. Indeed, bacterial or fungal infection up-regulated the expression of *Se-5HTR*. The increase of *Se-5HTR* expression might be explained by the up-regulation of *de novo* biosynthesis of its ligand, 5-HT, via increase in expression of biosynthetic genes as seen in hemocytes of *P. rapae* larvae after immune challenge[22].

The presence of 5-HT_7 receptor in hemocytes of *S. exigua* and its physiological function associated with immune responses were supported by its sensitivity to specific 5-HTR inhibitors. In response to 5-HT or bacterial challenge, *S. exigua* larvae exhibited significant increase of THC. This up-regulation of THC was explained by mobilization of sessile hemocytes to circulatory form by cytoskeletal rearrangement via a small G protein, Rac1[45,52]. This suggests that Se-5HTR can activate Rac1 to stimulate the hemocyte behavior. In vertebrates, activation of 5-HT_7 receptor increases cAMP level via a trimeric G protein G_s and small G proteins of Rho family including Cdc42, RhoA, and Rac1 via another trimeric G protein G_{12}[58]. This suggests that immune challenge can induce biosynthesis and release of 5-HT which then binds to Se-5HTR on hemocytes and activates Rac1 to stimulate hemocyte behaviors. In addition, the cAMP pathway triggered by Se-5HTR might activate Akt and ERK1/2 as seen in mammalian cancer cells[59] to facilitate actin rearrangement to form cellular shape change of hemocytes. These findings suggest that Se-5HTR plays a crucial role in hemocyte migration and cell shape change during cellular immune responses. Indeed, RNAi of *Se-5HTR* expression resulted in significant immunosuppression by exhibiting reduction in phagocytosis and nodulation. This was further supported by *Se-5HTR* knockout mutant

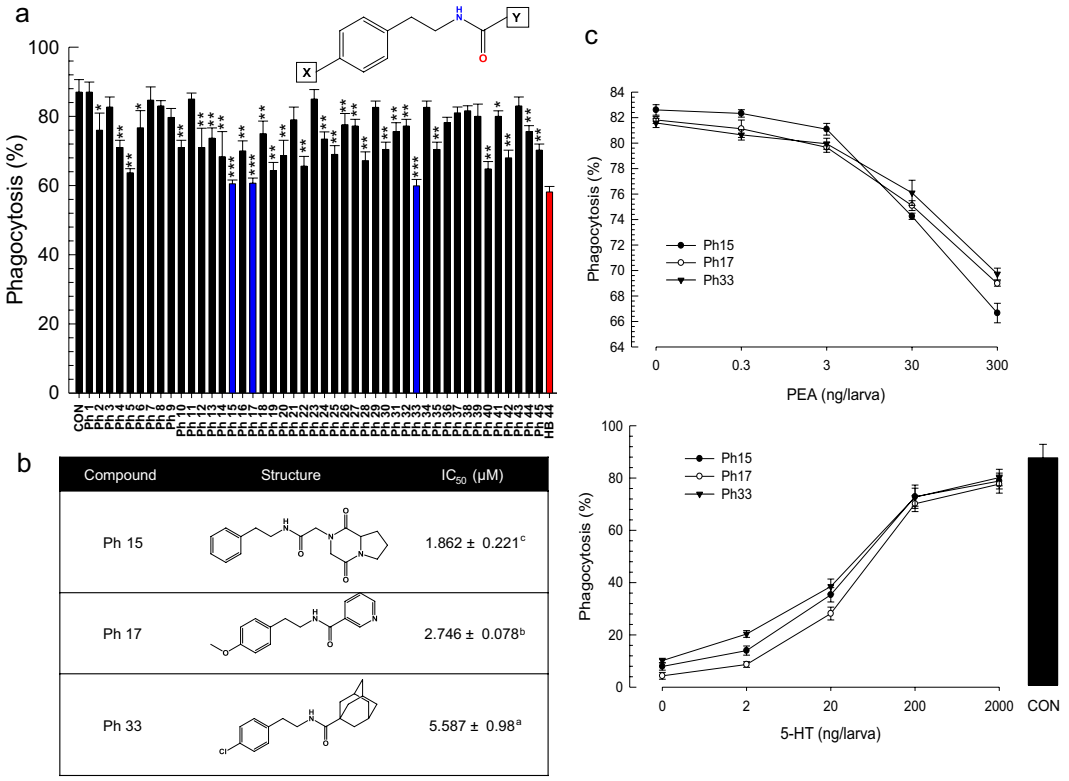

Figure 10. Validation of phenylethylamide (PEA) compounds for their inhibitory activities against 5-HTR using derivatives with different side chains ('X' and 'Y' of PEA skeleton). (**a**) Screening of 45 PEA derivatives for their effects on hemocyte phagocytosis of *S. exigua* with HB 44, a potent bacterial metabolite, as reference. PEA compounds (300 ng/larva) were injected into hemocoels of L5 larvae along with FITC-tagged bacteria. After incubating for 15 min, hemocytes were assessed for phagocytosis. Asterisks above standard deviation bars indicate significant difference compared to control ('CON' without inhibitor) at Type I error = 0.05 (*), 0.01 (**), and 0.005 (***) (LSD test). (**b**) Chemical structures of three selected PEA compounds and their median inhibitory doses (IC_{50}). (**c**) Competitive inhibition of the three selected PEA derivatives with 5-HT against Se-5HTR mediated phagocytosis. For dose-response analysis of inhibitory compounds (0, 0.3, 3, 30, and 300 ng/larva), a fixed 5-HT concentration (1 μg/larva) was used. For dose-response of 5-HT (0, 2, 20, 200 and 2,000 ng/larva), a fixed HB compound concentration (1 μg/larva) was used. 'CON' represents a positive control without any inhibitor.

generated by CRISPR-Cas9 technology. The mutant larvae suffered from poor phagocytotic activity even in the presence of 5-HT.

Bacterial metabolites derived from two entomopathogens, *Xenorhabdus* and *Photorhabdus*, inhibited cellular immune responses mediated by Se-5HTR. Especially, six chemical groups (phenylethylamide, tryptamide, xenortide, xenocycloin, nematophin, and GameXPeptide) highly inhibited both phagocytosis and nodulation, suggesting that they can inhibit Se-5HTR. This was supported by their competitive inhibition with the ligand, 5-HT. Bacterial secondary metabolites may be synthesized and released in the bacterium-nematode complex in order to defend immune attack from target insect to compete with other microbes occurring in the insect cadaver and facilitate host nematode development or bacterial quorum sensing[47]. It has been reported phenylethylamides and tryptamides identified from *Xenorhabdus* can act as quorum quenching activators by competitive binding to N-acylated homoserine lactone (AHL) receptor because AHL accumulation drives gene expression of bioluminescence, virulence factor, and biofilm formation in bacteria[60,61]. Xenortides are linear peptides consisting of 2–8 amino acids synthesized from both *Xenorhabdus* and *Photorhabdus*[62]. They are synthesized in insect hosts during infection with putative role in inhibiting prophenoloxidase activation to suppress insect immunity[63]. Xenocycloins produced by *X. bovienii* are cytotoxic to hemocytes of *Galleria melonella*[64]. Nematophin is synthesized by condensation of α-keto acid and tryptamine in *X. nematophila*. It possesses a specific antibacterial activity against *Staphylococcus aureus*[65]. GameXPeptides are cyclic pentapeptides widely synthesized in both *Xenorhabdus* and *Photorhabdus*. However, their biological functions remain unclear[66]. This current study showed that these six compound classes could inhibit cellular immune responses by competitive inhibition with 5-HT against Se-5HTR.

A novel phenylethylamide compound, PhX, was found to be highly inhibitory against Se-5HTR. Derivatives of phenylethylamide compound (HB 44) exhibited different inhibitory activities against cellular immune responses mediated by Se-5HTR. Especially, PhX containing methoxy and hexahydropyrrolo[1,2-α]pyrazine-1,4-dione

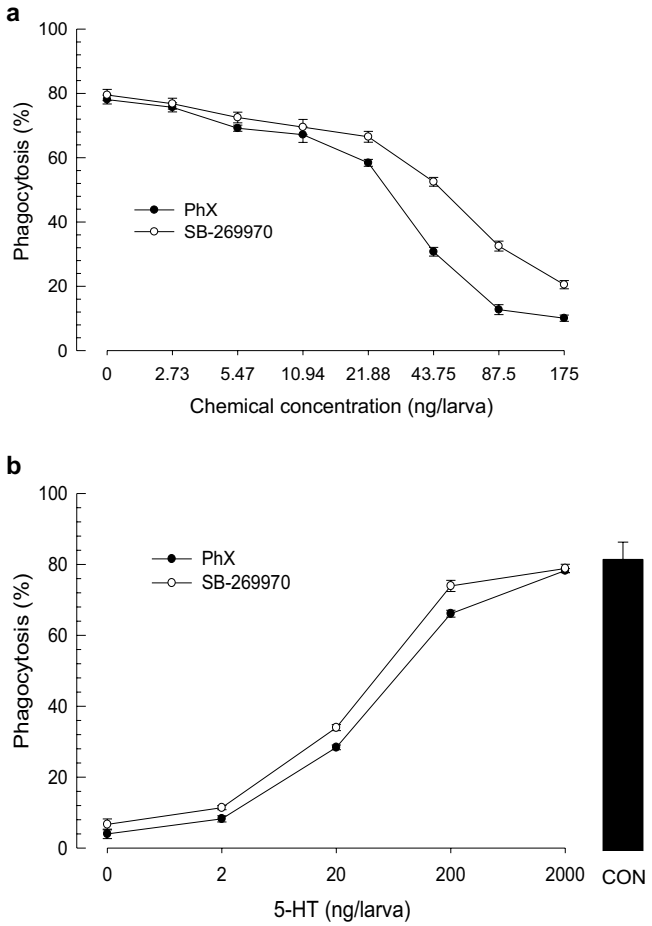

Figure 11. Specific inhibition of a designed compound (PhX) on Se-5HTR with a commercial 5-HTR_7 inhibitor (SB-269970) as reference in phagocytosis of *S. exigua*. FITC-tagged *E. coli* cells were injected to L5 larvae along with test chemicals. After 15 min, phagocytic cells were observed under a fluorescent microscope at 400 × magnification and percentage of phagocytotic hemocytes was calculated from randomly chosen 100 cells. Each treatment was independently replicated three times. (**a**) Dose-response of PhX and SB-269970 with a fixed 5-HT concentration (500 ng/larva). (**b**) Dose-response of 5-HT (0, 0.002, 0.02, 0.2, and 2 µg/larva) with a fixed inhibitor concentration (10 ng/larva). 'CON' represents a positive control without any inhibitor.

exhibited the highest inhibitory activity. 5-HT receptors have been used for screening for potent insecticides with growth-inhibiting or larvicidal activities against *Pseudaletia separata*[67]. Thus, PhX can be a candidate for this application unless it shows mammalian or non-target species toxicity[68].

Methods

Insect rearing and microbial culture. A laboratory strain of *S. exigua* was originated from Welsh onion field (Andong, Korea) and maintained for ~20 years. Larvae of this laboratory strain were reared on an artificial diet[69] at temperature of 25 ± 1 °C and relative humidity of 60 ± 10% with a photoperiod of 16:8 h (L:D). Under these conditions, larvae had five instars ('L1-L5'). Adults were reared with 10% sucrose solution. For immune challenge, *Escherichia coli* Top10 (Invitrogen, Carlsbad, CA, USA) was cultured in Luria-Bertani (LB) medium (BD Korea, Seoul, Korea) in a shaking incubator (200 rpm) at 37 °C overnight (16 h).

Chemicals. Serotonin hydrochloride was purchased from Sigma-Aldrich Korea (Seoul, Korea). It was dissolved in distilled water. SB-269970 (a specific inhibitor to 5-HT receptor subtype 7, 5-HT_7) was purchased from Cayman Chemical Company (Korea). It was dissolved in desired concentrations with dimethyl sulfoxide (DMSO). Fluorescein isothiocyanate (FITC) [2-(6-hydroxy-3-oxo-3h-xanthen-9-yl)-5-isothiocyanatobenzoic acid] was purchased from Sigma-Aldrich Korea. It was dissolved in DMSO to make a solution at 10 mg/mL. Anticoagulant buffer (ACB) was prepared using 98 mM NaOH, 186 mM NaCl, 17 mM Na_2EDTA, and 41 mM citric acid at pH 4.5. Phosphate-buffered saline (PBS) was prepared at pH 7.4 with 50 mM sodium phosphate and 0.7% NaCl. Tris-buffered saline (TBS) was prepared using 150 mM NaCl, 50 mM Tris-HCl at pH 7.6. Hank's balanced salt solution (HBSS) was prepared with the following compositions: 8 g NaCl, 400 mg KCl, 40 mg Na_2HPO_4, 60 mg KH_2PO_4, 1 g glucose, 140 mg $CaCl_2$, 120 mg $MgSO_4$, and 350 mg $NaHCO_3$ in 1,000 mL distilled H_2O.

Bioinformatics to search for 5-HT receptor and sequence analysis. *S. exigua* 5-HT receptor (Se-5HTR) sequence was obtained from GenBank by manual annotation. Briefly, a dopamine receptor sequence (AKR18180.1) of *Chilo suppressalis* was used to screen a transcriptome (SRR1050532) of *S. exigua*. A blast contig (GARL01017386.1) was analyzed for open reading frame (ORF) and the predicted amino acid sequence was used for analysis using BlastP program against GenBank (www.ncbi.nlm.nih.gov). After confirming its high homologies (E value $< 10^{-20}$) with other known insect 5HTRs, the resulting ORF sequence (=Se-5HTR) was deposited at NCBI-GenBank (accession number: MH025798). Sequence alignment was established using Clustal Omega tool (https://www.ebi.ac.uk/Tools/msa/clustalo/) provided by European Bioinformatics Institution. Phylogenetic tree was generated with Neighbor-joining method using Mega6 and ClustalW programs. Bootstrapping values were obtained with 1,000 repetitions to support branch and clustering. Protein domain was predicted using InterPro tool (https://www.ebi.ac.uk/interpro/), pfam (http://pfam.xfam.org), and Prosite (http://prosite.expasy.org/).

RNA extraction and cDNA preparation. Using Trizol reagent (Invitrogen), total RNAs were extracted from all developmental stages as well as larval tissues (hemocyte, midgut, fat body, and brain) of *S. exigua* according to the instruction of the manufacturer. Numbers of individuals used for RNA extraction for each individual developmental stage were as follows: ~500 eggs, ~20 larvae for L1-L2, ~10 larvae for L3, ~5 larvae for L4, one larva for L5, one pupa, and one adult. L5 larvae were used for RNA extraction from different tissue samples. After extraction, total RNAs were resuspended in nuclease-free water and cDNAs were synthesized from ~1 µg of RNAs using Maxime RT Premix (Intron Biotechnology, Seoul, Korea) according to the manufacturer's instruction.

Expression pattern of Se-5HTR by RT-qPCR. A fragment of *Se-5HTR* was amplified with gene-specific primers (5′-CTT TAC CTT CGT GTC TTC TC-3′ and 5′-GGT GTC AGT CTT CTC ATT AC-3′). PCR was performed with 35 cycles of denaturation (94 °C, 1 min), annealing (49 °C, 1 min), and extension (72 °C, 1 min). PCR products were subjected to agarose gel electrophoresis to visually confirm their amplifications. With the same gene-specific primers used in RT-PCR, RT-qPCR was performed in a qPCR machine (CFX Connect™ Real-Time PCR Detection System, Bio-Rad, Hercules, CA, USA) using SYBR Green Realtime PCR Master Mix (Toyobo, Osaka, Japan) under a guideline of Bustin *et al.*[70]. The amplification used 40 cycles of 15 s at 95 °C, 30 s at 60 °C, and 45 s at 72 °C. After PCR reactions, melting curves from 60 to 95 °C were obtained to confirm unique PCR products. A ribosomal protein, RL32, gene was used as a control with primers of 5′-ATG CCC AAC ATT GGT TAC GG-3′ and 5′-TTC GTT CTC CTG GCT GCG GA-3′. Each treatment was independently triplicated. Relative quantitative analysis method ($2^{-\Delta\Delta CT}$) was used to estimate mRNA expression levels of *Se-5HTR*.

RNA interference (RNAi). Gene fragment of *Se-5HTR* was amplified from template DNA using gene-specific primers (5′-CTT TAC CTT CGT GTC TTC TC-3′ and 5′-GGT GTC AGT CTT CTC AT-3′) possessing T7 RNA polymerase promoter sequence (5′-TAA TAC GAC TCA CTA TAG GGA GA-3′) at 5′ ends. PCR was performed with 5 cycles of denaturation (94 °C, 1 min), annealing (49 °C, 1 min), and extension (72 °C, 1 min) followed by 30 cycles of denaturation (94 °C, 1 min), annealing (60 °C, 1 min), and extension (72 °C, 1 min) to synthesize DNA template for dsRNA synthesis. Double-stranded RNA (dsRNA) against *Se-5HTR* ('dsSe-5HTR') was synthesized using Megascript RNAi kit (Ambion, Austin, TX, USA) following the manufacturer's instruction. The resulting dsRNA was blended with Metafectene PRO (Biontex, Plannegg, Germany) at 1:1 (v:v) ratio and incubated at 25 °C for 30 min for liposome formation. Two microliters of the prepared mixture containing ~900 ng of dsRNA was injected twice into *S. exigua* larval hemocoel using a microsyringe (Hamilton, Reno, NV, USA) equipped with a 26-gauge needle. The first injection was at late L4 stage. It was repeated 12 h afterwards. RNAi efficacy at 0, 24, and 48 h post-injection (PI) in reducing *Se-5HTR* expression was determined by RT-qPCR. At 24 h PI, treated larvae were used for immune challenge experiments. Each treatment was replicated thrice using 10 larvae for each replication.

Total hemocyte count (THC). Hemolymph was collected by cutting larval proleg and mixed with ACB (1:10, v/v). Hemocytes were counted using a Neubauer hemocytometer (Superior Marienfeld, Lauda-Königshofen, Germany) under a phase contrast microscope (BX41, Olympus, Tokyo, Japan) at 100 × magnification. Heat-killed (90 °C, 30 min) *Escherichia coli* (5×10^5 cells/larva) and a test chemical (5-HT or SB-269970) were co-injected into hemocoel through abdominal proleg of L5 larvae in a volume of 5 µL using a 10 µL micro-syringe (Hamilton) after surface-sterilization with 70% ethanol. After 4 h of incubation at 25 ± 2 °C, hemolymph of the insect was collected and assessed for THC.

Hemocyte-spreading analysis. After hemolymph (~150 µL) was collected from five L5 larvae by cutting prolegs, it was mixed with three times volume of ice-cold ACB and incubated on ice for 30 min. ACB-treated hemolymph was then centrifuged at 800 × *g* for 5 min at 4 °C. The resulting pellet was re-suspended in 500 µL of filter-sterilized TC-100 insect cell culture medium (Welgene, Daegu, Korea). On a glass coverslip placed in a moist chamber, 10 µL of hemocyte suspension was applied and placed in a dark condition. Hemocytes were then fixed with 4% paraformaldehyde (filter-sterilized) at 25 °C for 10 min and then washed thrice with filter-sterilized PBS. Cells were then permeabilized with 0.2% Triton-X dissolved in PBS at 25 °C for 2 min and washed with PBS. After that, hemocytes were blocked using 10% bovine serum albumin (BSA) dissolved in PBS at 25 °C for 10 min and washed again with PBS. Cells were then incubated with FITC-tagged phalloidin in PBS for 60 min and washed thrice with PBS. Hemocytes nuclei were then stained by incubating with 4′,6-diamidino-2-phenylindole (DAPI, 1 µg/mL) (Thermo Fisher Scientific, Rockford, IL, USA) dissolved in PBS and washed thrice with PBS. Hemocytes were then observed under a fluorescence microscope (DM2500, Leica, Wetzlar, Germany) at 400 × magnification. Hemocyte-spreading was dictated by appendages of F-actin outward the hemocyte cell boundary.

To assess effect of *Se-5HTR* RNAi on hemocyte-spreading, hemocytes were collected at 24 h after injecting dsSe-5HTR (~900 ng/larva). In separate experiments, 5-HT and 5-HTR inhibitor SB-269970 were co-injected

into dsRNA-treated larvae at ratios of 1:10 and 10:1 to check their influence on hemocyte-spreading. At 6 h after co-injection, hemolymph was collected from the treated larva and hemocyte-spreading was observed using the above-mentioned method.

Nodulation assay. Overnight culture of *E. coli* Top10 bacterial cells was washed with PBS and centrifuged at 1,120 × *g* for 10 min. L5 larvae were used to assess hemocyte nodule formation by immune-challenge with bacterial injection (~1.8×10^5 cells/larva) through the abdominal proleg into larval hemocoel using a microsyringe as previously described. To assess the effect of *Se-5HTR* RNAi on nodule formation, bacterial challenge was performed at 24 h after injecting dsSe-5HTR (~900 ng/larva). To check the influence of chemicals on nodule formation, 2 µg of ketanserin and/or 10 µg of 5-HT was co-injected along with the bacterial suspension. In separate experiment, 1 µg of the bacterial secondary metabolite was co-injected with the bacterial suspension to assess immune suppression activity of the test compound. After an incubation period of 8 h at 25 °C, treated insects were dissected under a stereo microscope (SZX9, Olympus, Japan) to count melanized nodule numbers. Each treatment was triplicated independently using five insects for each replication.

Phagocytosis assay. Preparation of FITC-labeled bacterial cells followed the method described by Harlow and Lane[71]. Briefly, *E. coli* Top10 cells were cultured in 50 mL of Luria-Bertani broth (37 °C, 16 h). These bacterial cells were then harvested by centrifuging 1 mL of the cultured broth at 1,120 × *g* for 10 min at 4 °C. Bacterial cells (10^5 cells/mL) were washed twice with TBS and re-suspended in 1 mL of 0.1 M sodium bicarbonate buffer (pH 9.0). In the suspension, 1 µL of 10 mg/mL FITC solution was added and immediately mixed. The mixture was then incubated in dark condition with end-over-end rotation at 25 °C for 30 min. After the incubation, FITC-tagged bacteria were harvested by centrifugation at 22,000 × *g* for 20 min at 4 °C. Bacterial cells were then washed thrice with HBSS to remove unbound dye and re-suspended in TBS.

To assess *in vivo* phagocytosis activity, 5 µL of FITC-tagged *E. coli* suspension was injected into the hemocoel of L5 larva through the proleg. To assess the effect of *Se-5HTR* RNAi on phagocytosis activity, bacteria were injected at 24 h after injecting dsSe-5HTR (~900 ng/larva). To check the influence of a specific 5-HT_7 receptor inhibitor on phagocytosis, 2 µg of SB-269970 was co-injected with the tagged bacterial suspension. To determine the effect of secondary metabolite on phagocytosis, 1 µg of bacterial secondary metabolite was co-injected with tagged bacterial suspension. After 15 min of incubation, treated larvae were surface-sterilized using 70% ethanol. With a pair of scissors, the proleg was cut to collect hemolymph sample (~50 µL) in 150 µL of cold ACB with gentle shaking of the tube to mix hemolymph and ACB thoroughly. Hemocyte monolayers were made using 50 µL of hemocyte suspension (~5×10^3 cells) and left in a moist chamber for 15 min for hemocytes to settle and attach to the glass surface. After the incubation period, monolayers were washed with TBS to remove plasma. These monolayers were overlaid with 1% trypan blue dye solution to quench non-phagocytosed bacterial cells. After 10 min, monolayers were washed again with TBS and then fixed with 1.5% glutaraldehyde solution to observe under a fluorescence microscope at 400× magnification. Hemocytes undergoing phagocytosis were counted from a total of 100 hemocytes observed from different areas of each slide. Each observation was triplicated with three different slides.

Preparation of Se-5HTR knockout mutant using CRISPR-Cas9. A guide RNA sequence for CRISPR-Cas9 technology against *Se5HTR* was designed by a CRISPR guide RNA analysis tool CHOPCHOP (https://chopchop.rc.fas.harvard.edu). Single-stranded guide RNA (sgRNA) was synthesized using a PCR-based technique following the manufacturer's protocol (Guide-it sgRNA *In Vitro* Transcription Kit, Takara Bio USA, Mountain View, CA, USA). Briefly, a forward oligonucleotide (CGT GCG CCA TCA TCG CGC TG) was mixed with Guide-it Scaffold template and performed PCR at 98 °C for 5 s, 33 cycles (98 °C for 10 s and 68 °C for 10 s) to generate sgRNA DNA template. After confirming the single band at ~130 bp, *in vitro* transcription reaction was performed to generate sgRNA.

For injection to eggs, newly (<1 h) laid eggs was kept in desiccator for 10 min and fixed onto a glass slide with double-sided tape. Injection needle was prepared by pulling siliconized 10 µL quartz microcapillaries using a horizontal micropipette puller (Narishige, Tokyo, Japan) and beveled with a BV-10 beveller (Narishige). The fixed eggs were injected with 5 nL of a mixture containing 500 ng/µL of recombinant Cas9 nuclease and 50 ng/µL of target-specific sgRNA using a micromanipulator (PN-30, Narishige) under a stereo microscope (SZX9, Olympus Corporation, Japan) equipped with a mechanical stage. Eggs were incubated at 27 °C until hatching.

To assess the mutation in the target DNA site, genomic DNA was extracted using 5% Chelex 100 resin (BioRad, Hercules, CA, USA) from hemolymph of L5 larvae. The PCR conditions were as follows: 98 °C for 2 min, followed by 35 cycles of 94 °C for 30 s, 49 °C for 1 min, and 72 °C for 1 min, followed by a final extension period of 72 °C for 10 min. The PCR products were then cloned into the pCR2.1 vector (ThermoFisher Scientific Korea, Seoul, Korea) and bidirectionally sequenced.

Preparation of organic extracts from bacterial culture broth. *X. nematophila* K1 (Xn) and *P. temperata temperata* ANU101 (Ptt) bacteria were cultured in TSB at 28 °C for 48 h. Culture broths were centrifuged at 12,500 × *g* for 30 min and supernatants were used for subsequent fractionation. To obtain ethyl acetate extract, the same volume (1 L) of ethyl acetate was mixed with the supernatant and separated into organic and aqueous fractions. Ethyl acetate extract ('EAX') was dried using a rotary evaporator (Sunil Eyela, Seongnam, Korea) at 40 °C. The resulting extract (0.2 mg) was obtained from 1 L cultured broth and resuspended with 5 mL of methanol. The aqueous phase was then combined with 1 L of butanol. Butanol extract ('BX') was also dried using the rotary evaporator at 40 °C and the resulting extract (0.2 mg) was resuspended with 5 mL of methanol.

Secondary bacterial metabolites – biological activity against immune responses. Secondary metabolites (37 samples, Supplementary Fig. 4) derived from *Xenorhabdus* and *Photorhabdus* cultures were from

the Bode lab compound collection named 'HB' compounds. Their biological activities for suppressing *S. exigua* immunity were then determined. Individual chemicals were dissolved in DMSO, diluted into desired concentrations with DMSO, and stored at −20 °C.

For hemocyte nodulation inhibition assay, overnight culture of *E. coli* bacterial cells was washed with PBS. Test compound (1 µg/larva) was injected into larval hemocoel along with the bacterial suspension (~1.8×10^5 cfu/larva) using a microsyringe as previously described. Insects were then incubated at 25 °C for 8 h. After the incubation period, insects were dissected and nodule numbers were counted as described above. Each treatment was triplicated independently using five insects for each replication. For phagocytosis inhibition assay, 5 µL of FITC-tagged *E. coli* suspension along with 1 µg of test compound was injected into L5 larval hemocoel. After 15 min of incubation period, hemocytes undergoing phagocytosis were counted as previously described.

Secondary bacterial metabolites – competitive assay with 5-HT. To determine effects of bacterial secondary metabolites on nodulation and phagocytosis, 10 potent chemicals were selected based on their common inhibitory activity on both phagocytosis and nodulation and their median inhibition concentration (IC_{50}) values were calculated. Percentages of phagocytosis against increasing concentrations of HB chemicals were calculated and their IC_{50} values were calculated using Probit analysis (https://probitanalysis.wordpress.com). To assess a competitive inhibitory activity between test compound and 5-HT, HB chemicals were injected in different doses (0, 0.01, 0.1, 1 and 10 µg/larva) along with a fixed 5-HT concentration (1 µg/larva) and FITC-tagged bacteria (500 cells/larva). In a separate experiment, different doses of 5-HT were injected into the larvae with a fixed HB compound content (1 µg/larva). At 15 min after bacterial injection, hemocytes from treated larvae were collected in ACB and phagocytosis assay was performed as described above.

Chemical derivatives and their inhibitory activities against Se-5HTR. Based on potent phenylethylamide (PEA) HB compounds, 45 additional PEA samples (Supplementary Fig. 5) were obtained from Korea Chemical Bank of the Korea Research Institute of Chemical Technology (KRICT). Derivative compounds were dissolved in DMSO, diluted into desired concentrations with DMSO, and stored at −20 °C. These PEA chemicals were then tested for their abilities to suppress nodule formation and phagocytosis in *S. exigua* as described above. For nodulation inhibition assay, each chemical (150 ng/larva) was injected into larval hemocoel along with bacterial suspension (~1.8×10^5 cfu/larva). Each treatment was triplicated independently using five insects for each replication. For phagocytosis inhibition assay, 5 µL of FITC-tagged *E. coli* suspension along with 150 ng of each chemical was injected into L5 larval hemocoel of *S. exigua*. After incubating for 15 min, hemocytes undergoing phagocytosis were counted using previously described method.

Chemical synthesis of PhX. A potent chemical was designed as PhX ((*S*)-2-(1,4-dioxohexahydropyrrolo[1,2-α]pyrazin-2(1*H*)-yl)-*N*-(4-methoxyphenethyl)acetamide) and chemically synthesized according to a method described in Supplementary Fig. 6.

Statistical analysis. All studies were triplicated independently. Results are expressed as mean ± standard error. Results were plotted using Sigma plot (Systat Software, San Jose, CA, USA). Means were compared by least squared difference (LSD) test of one-way analysis of variance (ANOVA) using POC GLM of SAS program[72] and discriminated at Type I error = 0.05.

Received: 17 July 2019; Accepted: 16 December 2019;
Published online: 30 December 2019

References

1. Roshchina, V. V. New trends and perspectives in the evolution of neurotransmitters in microbial, plant, and animal cells. *Adv. Exp. Med. Biol.* **874**, 25–77 (2016).
2. Lovenberg, W., Weissbach, H. & Udenfriend, S. Aromatic L-amino acid decarboxylase. *J. Bio.l Chem.* **237**, 89–93 (1962).
3. Hufton, S. E., Jennings, I. G. & Cotton, R. G. Structure and function of the aromatic amino acid hydroxylases. *Biochem. J.* **311**, 353–66 (1995).
4. Roberts, K. M. & Fitzpatrick, P. F. Mechanisms of tryptophan and tyrosine hydroxylase. *IUBMB Life* **65**, 350–357 (2013).
5. Zhang, X., Beaulieu, J. M., Sotnikova, T. D., Gainetdinov, R. R. & Caron, M. G. Tryptophan hydroxylase-2 controls brain serotonin synthesis. *Science* **305**, 217 (2004).
6. Gershon, M. D. & Tack, J. The serotonin signaling system: from basic understanding to drug development for functional GI disorders. *Gastroenterology* **132**, 397–414 (2007).
7. Richtand, N. M. & McNamara, R. K. Serotonin and dopamine interactions in psychosis prevention. *Prog. Brain Res.* **172**, 141–153 (2008).
8. Monti, J. M. Serotonin control of sleep-wake behavior. *Sleep Med. Rev.* **15**, 269–281 (2011).
9. Švob Štrac, D., Pivac, N. & Mück-Šeler, D. The serotonergic system and cognitive function. *Transl. Neurosci.* **7**, 35–49 (2016).
10. Seuwen, K. & Pouysségur, J. Serotonin as a growth factor. *Biochem. Pharmacol.* **39**, 985–990 (1990).
11. Li, N., Wallén, N. H., Ladjevardi, M. & Hjemdahl, P. Effects of serotonin on platelet activation in whole blood. *Blood Coagul. Fibrinolysis* **8**, 517–23 (1997).
12. Hayashi, K. *et al.* Serotonin attenuates biotic stress and leads to lesion browning caused by a hypersensitive response to *Magnaporthe oryzae* penetration in rice. *Plant J.* **85**, 46–56 (2016).
13. Majeed, Z. R. *et al.* Modulatory action by the serotonergic system: behavior and neurophysiology in *Drosophila melanogaster*. *Neural Plast.* **2016**, 1–23 (2016).
14. Huser, A. *et al.* Anatomy and behavioral function of serotonin receptors in *Drosophila melanogaster* larvae. *PLoS One* **12**, e0181865 (2017).
15. Becnel, J., Johnson, O., Luo, J., Nässel, D. R. & Nichols, C. D. The serotonin 5-HT_{7Dro} receptor is expressed in the brain of *Drosophila*, and is essential for normal courtship and mating. *PLoS One* **6**, e20800 (2011).
16. Yuan, Q., Lin, F., Zheng, X. & Sehgal, A. *Serotonin modulates circadian entrainment in Drosophila*. *Neuron. 2005;* **47**, 115–127 (2005).
17. Nichols, C. D. 5-HT_2 receptors in *Drosophila* are expressed in the brain and modulate aspects of circadian behaviors. *Dev. Neurobiol.* **67**, 752–763 (2007).

18. Yuan, Q., Joiner, W. J. & Sehgal, A. A sleep-promoting role for the *Drosophila* serotonin receptor 1A. *Curr. Biol.* **16**, 1051–1062 (2016).
19. Neckameyer, W. S., Coleman, C. M., Eadie, S. & Goodwin, S. F. Compartmentalization of neuronal and peripheral serotonin synthesis in *Drosophila melanogaster*. *Genes Brain Behav.* **6**, 756–769 (2007).
20. Dierick, H. A. & Greenspan, R. J. Serotonin and neuropeptide F have opposite modulatory effects on fly aggression. *Nat. Genet.* **39**, 678–682 (2007).
21. Kaplan, D. D., Zimmermann, G., Suyama, K., Meyer, T. & Scott, M. P. A nucleostemin family GTPase, NS3, acts in serotonergic neurons to regulate insulin signaling and control body size. *Genes Dev.* **22**, 1877–1893 (2008).
22. Qi, Y. X. *et al*. Serotonin modulates insect hemocyte phagocytosis via two different serotonin receptors. *Elife* **5**, e12241 (2016).
23. Python, F. & Stocker, R. F. Immunoreactivity against choline acetyltransferase, gamma-aminobutyric acid, histamine, octopamine, and serotonin in the larval chemosensory system of *Drosophila melanogaster*. *J. Comp. Neurol.* **453**, 157–167 (2016).
24. Dasari, S. & Cooper, R. L. Direct influence of serotonin on the larval heart of *Drosophila melanogaster*. *J. Comp. Physiol. B.* **176**, 349–357 (2006).
25. Rodriguez, M. V. G. & Campos, A. R. Role of serotonergic neurons in the *Drosophila* larval response to light. *BMC Neurosci.* **10**, 66 (2009).
26. Barnes, N. M. & Sharp, T. A review of central 5-HT receptors and their function. *Neuropharmacology* **38**, 1083–1152 (1999).
27. Nichols, D. E. & Nichols, C. D. Serotonin receptors. *Chem. Rev.* **108**, 1614–1641 (2008).
28. Roth, B. L. The serotonin receptors: from molecular pharmacology to human therapeutics. *Humana Press*, *Totowa*, *New Jersey* (2006).
29. Thompson, A. J. & Lummis, S. C. R. 5-HT_3 Receptors. *Curr. Pharm. Des.* **12**, 3615–3630 (2006).
30. Watanabe, T., Sadamoto, H. & Aonuma, H. Identification and expression analysis of the genes involved in serotonin biosynthesis and transduction in the field cricket *Gryllus bimaculatus*. *Insect Mol. Biol.* **20**, 619–635 (2011).
31. Ono, H. & Yoshikawa, H. Identification of amine receptors from a swallowtail butterfly, *Papilio xuthus* L.: cloning and mRNA localization in foreleg chemosensory organ for recognition of host plants. *Insect Biochem. Mol. Biol.* **34**, 1247–1256 (2004).
32. Vleugels, R., Lenaerts, C., Baumann, A., Vanden, B. J. & Verlinden, H. Pharmacological characterization of a 5-HT_1-type serotonin receptor in the red flour beetle, *Tribolium castaneum*. *PLoS One* **8**, e65052 (2013).
33. Troppmann, B., Balfanz, S., Baumann, A. & Blenau, W. Inverse agonist and neutral antagonist actions of synthetic compounds at an insect 5-HT_1 receptor. *Br. J. Pharmacol.* **159**, 1450–1462 (2010).
34. Guo, X., Ma, Z. & Kang, L. Serotonin enhances solitariness in phase transition of the migratory locust. *Front. Behav. Neurosci.* **7**, 129 (2013).
35. Qi, Y. X. *et al*. Larvae of the small white butterfly, *Pieris rapae*, express a novel serotonin receptor. *J. Neurochem.* **131**, 767–777 (2014).
36. Qi, Y. X. *et al*. Characterization of three serotonin receptors from the small white butterfly, *Pieris rapae*. *Insect Biochem. Mol. Biol.* **87**, 107–116 (2017).
37. Thamm, M., Balfanz, S., Scheiner, R., Baumann, A. & Blenau, W. Characterization of the 5-HT_{1A} receptor of the honeybee (*Apis mellifera*) and involvement of serotonin in phototactic behavior. *Cell Mol. Life Sci.* **67**, 2467–2479 (2010).
38. Schlenstedt, J., Balfanz, S., Baumann, A. & Blenau, W. Am5-HT_7: molecular and pharmacological characterization of the first serotonin receptor of the honeybee (*Apis mellifera*). *J. Neurochem.* **98**, 1985–1998 (2006).
39. Berridge, M. J. & Patel, N. Insect salivary glands - stimulation of fluid secretion by 5-hydroxytryptamine and adenosine-3′, 5′-monophosphate. *Science* **162**, 462–463 (1968).
40. Berridge, M. J. The role of 5-hydroxytryptamine and cyclic AMP in the control of fluid secretion by isolated salivary glands. *J. Exp. Biol.* **53**, 171–186 (1970).
41. Vanhoenacker, P., Haegeman, G. & Leysen, J. E. 5-HT_7 receptors: current knowledge and future prospects. *Trends Pharmacol. Sci.* **21**, 70–77 (2007).
42. Molaei, G. & Lange, A. B. The association of serotonin with the alimentary canal of the African migratory locust, *Locusta migratoria*: distribution, physiology and pharmacological profile. *J. Insect Physiol.* **49**, 1073–1182 (2003).
43. Baines, D., DeSantis, T. & Downer, R. G. H. Octopamine and 5-hydroxytryptamine enhance the phagocytic and nodule formation activities of cockroach (*Periplaneta americana*) haemocytes. *J. Insect Physiol.* **38**, 905–914 (1992).
44. Kim, K., Madanagapol, N., Lee, D. & Ki, Y. Octopamine and 5-hydroxytryptamine mediate hemocytic phagocytosis and nodule formation via eicosanoids in the beet armyworm, *Spodoptera exigua*. *Arch. Insect Biochem. Physiol.* **90**, 162–176 (2009).
45. Kim, G. S. & Kim, Y. Up-regulation of circulating hemocyte population in response to bacterial challenge is mediated by octopamine and 5-hydroxytryptamine via Rac1 signal in *Spodoptera exigua*. *J. Insect Physiol.* **56**, 559–566 (2010).
46. Kim, Y., Ji, D., Cho, S. & Park, Y. Two groups of entomopathogenic bacteria, *Photorhabdus* and *Xenorhabdus*, share an inhibitory action against phospholipase A_2 to induce host immunodepression. *J. Invertebr. Pathol.* **89**, 258–264 (2005).
47. Shi, Y. M. & Bode, H. B. Chemical language and warfare of bacterial natural products in bacteria-nematode-insect interactions. *Nat. Prod. Rep.* **35**, 309–335 (2018).
48. Tobias, N. J., Shi, Y. M. & Bode, H. B. Refining the natural product repertoire in entomopathogenic bacteria. *Trends Microbiol.* **26**, 833–840 (2018).
49. Barak, L. S. *et al*. A highly conserved tyrosine residue in G protein-coupled receptors is required for agonist-mediated ß2-adrenergic receptor sequestration. *J. Biol. Chem.* **269**, 2790–2795 (1994).
50. Ji, T. H., Grossmann, M. & Ji, I. G protein-coupled receptors. I. Diversity of receptor-ligand interactions. *J. Biol. Chem.* **273**, 17299–17302 (1998).
51. Huang, E. S. Construction of a sequence motif characteristic of aminergic G protein-coupled receptors. *Protein Sci.* **12**, 1360–1367 (2003).
52. Park, J., Stanley, D. & Kim, Y. Rac1 mediates cytokine-stimulated hemocyte spreading via prostaglandin biosynthesis in the beet armyworm, *Spodoptera exigua*. *J. Insect Physiol.* **59**, 682–689 (2013).
53. Venkatakrishnan, A. J. *et al*. Molecular signatures of G-protein-coupled receptors. *Nature* **494**, 185–194 (2013).
54. Ho, B. Y., Karschin, A., Branchek, T., Davidson, N. & Lester, H. A. The role of conserved aspartate and serine residues in ligand binding and in function of the 5-HT_{1A} receptor: A site-directed mutation study. *FEBS Lett.* **312**, 259–262 (1992).
55. Shapiro, D. A., Kristiansen, K., Weiner, D. M., Kroeze, W. K. & Roth, B. L. Evidence for a model of agonist-induced activation of 5-hydroxytryptamine 2A serotonin receptors that involves the disruption of a strong ionic interaction between helices 3 and 6. *J. Biol. Chem.* **277**, 11441–11449 (2002).
56. Qanbar, R. & Bouvier, M. Role of palmitoylation/depalmitoylation reactions in G-protein-coupled receptor function. *Pharmacol. Ther.* **97**, 1–33 (2003).
57. Romero, G., von Zastrow, M. & Friedman, P. A. Role of PDZ proteins in regulating trafficking, signaling, and function of GPCRs: means, motif, and opportunity. *Adv. Pharmacol.* **62**, 279–314 (2011).
58. Guseva, D., Wirth, A. & Ponimaskin, E. Cellular mechanisms of the 5-HT_7 receptor-mediated signaling. *Front. Behav. Neurosci.* **8**, 306 (2014).
59. Choi, C. & Helfman, D. M. The Ras-ERK pathway modulates cytoskeleton organization, cell motility and lung metastasis signature genes in MDA-MB-231 LM2. *Oncogene* **33**, 3668–3676 (2014).
60. Papenfort, K. & Bassler, B. L. Quorum sensing signal-response systems in Gram-negative bacteria. *Nat. Rev. Microbiol.* **14**, 576–588 (2016).

61. Bode, E. *et al*. Biosynthesis and function of simple amides in *Xenorhabdus doucetiae*. *Environ. Microbiol.* **19**, 4564–4575 (2017).
62. Reimer, D., Nollmann, F. I., Schultz, K., Kaiser, M. & Bode, H. B. Xenortide biosynthesis by entomopathogenic *Xenorhabdus nematophila*. *J. Nat. Prod.* **77**, 1976–1980 (2014).
63. Bloudoff, K. & Schmeing, T. M. Structural and functional aspects of the nonribosomal peptide synthetase condensation domain superfamily: discovery, dissection and diversity. *Biochim. Biophys. Acta* **1865**, 1587–1604 (2017).
64. Proschak, A. *et al*. Biosynthesis of the insecticidal xenocyloins in *Xenorhabdus bovienii*. *Chembiochem.* **15**, 369–372 (2014).
65. Li, J., Chen, G. & Webster, J. M. Nematophin, a novel antimicrobial substance produced by *Xenorhabdus nematophilus* (Enterobactereaceae). *Can. J. Microbiol.* **43**, 770–773 (1997).
66. Nollmann, F. I. *et al*. Insect-specific production of new GameXPeptides in *Photorhabdus luminescens* TTO1, widespread natural products in entomopathogenic bacteria. *Chembiochem.* **16**, 205–208 (2015).
67. Cai, M. *et al*. Design and synthesis of novel insecticides based on the serotonergic ligand 1-[(4-Aminophenyl) ethyl]-4-[3-(trifluoromethyl) phenyl] piperazine (PAPP). *J. Agric. Food Chem.* **58**, 2624–2629 (2009).
68. Verlinden, H., Vleugels, R. & Broeck, J. V. Serotonin, serotonin receptors and their actions in insects. *Neurotransmitter* **2**, e314 (2015).
69. Shrestha, S., Stanley, D. & Kim, Y. PGE_2 induces oenocytoid cell lysis via a G protein-coupled receptor in the beet armyworm, *Spodoptera exigua*. *J. Insect Physiol.* **57**, 1568–1576 (2011).
70. Bustin, S. A. *et al*. The MIQE guidelines: minimum information for publication of quantitative real-time PCR experiments. *Clin. Chem.* **55**, 4 (2009).
71. Harlow, E. & Lane, D. Labeling antibodies with fluorochromes. In: Using Antibodies. Cold spring harbor laboratory press, New York, pp. 85–87 (1988).
72. SAS Institute. SAS/STAT user's guide. SAS Institute, Inc., Cary, NC (1989).

Acknowledgements

This work was supported by a grant (No. 2017R1A2133009815) of the National Research Foundation (NRF) funded by the Ministry of Science, ICT and Future Planning, Republic of Korea. This work was also supported by a project (No SI1808, Development of crop protection agents leading the future market). The chemical library used in this research was provided by Korea Chemical Bank (http://www.chembank.org) of the Korea Research Institute of Chemical Technology (KRICT). We appreciate Youngim Song for ordering and arranging materials and Malsook Cho for rearing insects. Work in the Bode lab was supported by the LOEWE Center Translational Biodiversity Genomics funded by the state of Hesse, Germany.

Author contributions

A.H. and Y.K. performed the experiments and analyzed the data. Y.K. conceived and supervised the experiments. H.S.Y., J.R. and H.B. provided bacterial metabolites and derivative compounds. A.H. and Y.K. wrote the paper with contributions of H.S.Y., J.R. and H.B.

Competing interests

The authors declare no competing interests.

Additional information

Supplementary information is available for this paper at https://doi.org/10.1038/s41598-019-56892-z.

Correspondence and requests for materials should be addressed to Y.K.

Reprints and permissions information is available at www.nature.com/reprints.

Publisher's note Springer Nature remains neutral with regard to jurisdictional claims in published maps and institutional affiliations.